Synthesis, Antibacterial Activity and *Insilco* Studies of 1-(2-ethyl acetate)-2-styryl 5-nitroimidazole Derivatives.

By: Misgana Aragaw (BPharm)

Advisors: Dr. Solomon Tadesse (PhD.)

Dr. Daniel Bisrat (PhD.)

Dr. Mekonnen Abebayehu (PhD.)

A thesis Submitted to the Department of Pharmaceutical Chemistry and Pharmacognosy Presented in Partial Fulfillment of the Requirements for the Master of Science Degree in Medicinal Chemistry

June, 2023

Addis Ababa, Ethiopia

ADDIS ABABA UNIVERSITY

SCHOOL OF GRADUATE STUDIES

This is to certify that the thesis prepared by Misgana Aragaw, entitled: "*Synthesis, antibacterial activity and Insilco studies of 1-(2-ethyl acetate)-2-styryl 5-nitroimidazole derivatives*" and submitted in partial fulfillment of the requirements for the Degree of Master of Science in Medicinal Chemistry complies with the regulations of the university and meets the accepted standards with respect to originality and quality.

Signed by the Examining Committee:

External examiner: Dr. Kibrom Gebrehiwet Signature_____ Date_____

Internal examiner: Mr.Biniam Paulos Signature_____ Date_____

Dr. Solomon Tadesse (Advisor) Signature_____ Date_____

Dr. Daniel Bisrat (Advisor) Signature_____ Date_____

Dr. Mekonnen Abebayehu (Advisor) Signature_____ Date_____

_____

Chair of the Department

Abstract

Synthesis, antibacterial activity and *In silco* studies of 1-(2-ethyl acetate)-2-styryl 5- nitroimidazole derivatives.

By: Misgana Aragaw

The proliferation of drug-resistant microorganisms that have acquired new resistance mechanisms contributes to the development of antimicrobial resistance. For more than 60 years, metronidazole (**2**) has served as an antibacterial and antiprotozoal agent. However, its prolonged usage has resulted in drug-resistance and associated with adverse effects. Metronidazole is usually not effective on Gram-negative and Gram-positive facultative anaerobic bacteria, which are considered as the most life-threatening pathogens. However, there are reports of metronidazole analogues with potent activity against the facultative anaerobic bacteria indicate that there is a different mode of action of metronidazole. As a result, it is important to synthesize new metronidazole analogs with unique mode of action in order to enhance the antibacterial efficacy of metronidazole while reducing toxicity. Recent studies have shown that the enzyme FabH (β-ketoacyl-acyl carrier protein synthase III), responsible for the first step of fatty acid biosynthesis (FAB), is a promising target for nitroimidazole derivatives that can be used as an effective anti-infective. In this study, we synthesized four 2-styryl 5-nitroimidazoles derivatives, via condensation of metronidazole with respective benzaldehydes and subsequent acetylation reactions. The chemical structures of the synthesized compounds were determined through ^{1}H and ^{13}C-NMR spectroscopy. We evaluated the antimicrobial activity of the synthesized compounds against six bacterial strains, three Gram- positive bacterial strains (*S. aureus*, *S. epidermidus* and *S. agalactiae)* and three Gram-negative bacterial strains (*E. coli*, *P. aeruginosa* and *K. pneumoniae*) using a two-fold serial dilution MTT assay. Of all the

synthesized compounds, compound **33**, ((*E*)-2-(5-nitro-2-styryl-1H-imidazol-1-yl)ethyl acetate) and **36**, ((*E*)-2-(2-(4-(dimethylamino)styryl)-5-nitro-1H-imidazol-1-yl)ethyl acetate) equally demonstrated the most potent antibacterial activity against *S. agalactiae* (MIC = 1.56 μg/mL), *P. aeruginosa* (3.13 μg/mL), respectively. Additionally, compound **33** and **36** also exhibited potent activity against *K. pneumonia*, with an MIC value of 6.25 μg/mL and 12.5 μg/mL, respectively. Molecular docking studies revealed that both compounds have favorable hydrophobic and electrostatic interactions with conserved residues in the binding site of *E. coli* FabH -CoA complex (1HNJ.pdb). Overall acetylation of 2-styryl-5-nitroimidazoles improved both their biological activity and binding interaction with the target protein.

Key words: *Antibacterial activity, 2-styryl 5-nitroimidazoles, β-Ketoacyl-acyl carrier protein synthase III (FabH)*

Acknowledgments

First and foremost, I would like to acknowledge the Almighty GOD for blessing me with good health, strength, and resilience throughout my life's journey.

I would like to express my profound and sincere gratitude to my advisor, Dr. Solomon Tadesse, for his kind approach and genuine help with incredible encouragement and provision of constructive comments while preparing this thesis. I also extend my thanks to Dr. Mekonnin Abebayehu and Dr. Daniel Bisrat (PhD), my co-advisors, for their continuous support and valuable comments throughout this research study.

I am grateful to the Department of Chemistry, Addis Ababa University, for their help in characterization of compounds. Special thanks to Dr. Kibrom Gebreheiwot Bedane for his unreserved assistance and providing the necessary resources. I would like to acknowledge Mr. Sileshi Degu and Mr. Abiy Abebe at Ethiopian Public Health Institute (EPHI) for their cooperation and the facilities provided for conducting the biological experiment. I also would like to thank the Department of Pharmaceutical Chemistry and Pharmacognosy for the opportunity I have got to proceed in the research area I am highly interested.

To my family; friends; my sincere appreciation goes out to all who have contributed to the successful completion of this research work.

Table of Contents

List of Figures

List of Tables

Abbreviations

^{13}C NMR	Carbon Thirteen Nuclear Magnetic Resonance
^{1}H NMR	Proton Nuclear Magnetic Resonance
ATCC:	American Type Culture Collection
CFU:	Colony Forming Unit
CLSI:	Clinical and Laboratory Standards Institute
DEPT	Distortionless Enhancement by Polarization Transfer
DMSO	Dimethylsulfoxide
EPHI	Ethiopian Public Health Institute
FT-NMR	Furrier Transformed Nuclear Magnetic Resonance
HERG-	human ether-a-go-go related gene potassium channel
IC_{50}	Half maximal inhibitory concentration
MDCK	Madin-Darby canine kidney
MHB	Mueller Hinton Broth
MIC	Minimum inhibitory concentration
MTT	Methyl Tetrazolium Chloride
WHO	World Health Organization

1 Introduction

1.1 Infectious disease

1.1.1. Overview of infectious disease

Infectious diseases are a primary cause of death worldwide, particularly in low-income countries and among young children. A recent study titled "Global Comprehensive Estimates of the Burden of Bacterial Infections" by Ikuta *et al*. (2022) found that bacterial infections were responsible for 7.7 million deaths globally in 2019, making them the second leading cause of death. The top five pathogens causing these deaths were *Pseudomonas aeruginosa, Streptococcus pneumoniae, Escherichia coli, Klebsiella pneumoniae, and Staphylococcus aureus*, which acoounted for 54.9% of deaths (Ikuta *et al*., 2022). Mortality rates associated with these bacterial pathogens were highest in sub-Saharan African countries, signifying 230 deaths per 100 000 population and in the lowest in high-income countries, accounting for 52.2 deaths per 100 000 population. *S. aureus* was the most common bacterial cause of mortality across 135 nations, killing more people over the age of 15 than any other pathogen. *S. pneumoniae* was the pathogen most frequently linked to mortality in children under the age of five. More than six million people died in 2019 as a result of three bacterial infectious disorders, with lower respiratory infections and bloodstream infections causing 2 million of those deaths (Ikuta *et al*., 2022). Diarrheal, lower respiratory infections, tuberculosis, HIV/AIDS, were among the leading causes of premature mortality in 2019 in Ethiopia (Misganaw *et al*., 2022).

1.1.2. Drug-resistance bacteria

Antimicrobial resistance (AMR) is also becoming more of a worry, with the creation and spread of organisms that have developed new resistance mechanisms, threatening our capacity to treat common diseases. According to the World Health Organization

(WHO, 2021) , multi- and pan-resistant bacteria, popularly known as "superbugs," are quickly proliferating, producing diseases that are not curable with current antimicrobial medications. According to the study “Global Burden of Bacterial Antimicrobial Resistance” by Murray *et al*. (2022), bacterial AMR was associated with 4.95 million deaths in 2019, including 1.27 million attributable to bacterial AMR. For instance, the highest death rate attributable to microbial resistance was recorded in western sub-Saharan Africa, at 27.3 deaths per 100 000. Lower respiratory infections were the most burdensome infectious syndrome, accounting for more than 1.5 million deaths associated with resistance in 2019. *Escherichia coli* was the leading pathogens causing deaths associated with resistance, followed by followed by *Staphylococcus aureus, Klebsiella pneumoniae, Streptococcus pneumoniae, Acinetobacter baumannii,* and *Pseudomonas aeruginosa*. These bacteria were responsible for an estimated 3.57 million deaths attributed to AMR in 2019. There is also a high prevalence of antimicrobial resistance in Ethiopia, where commonly occurring pathogens such as Enterococcus species*, S. aureus, E. coli, K. pneumonia,* and *P. aeruginosa* are frequently resistant to key antimicrobial agents, according to a study conducted by Berhe *et al*, (2021).

1.2 Statement of the problem

Multi-drug resistant microorganisms such as *S. epidermidis, S. aureus, P. aeruginosa, E. coli, E. faecium, and S. apiospernum* pose a significant global threat to human health. Antibiotics commonly used to treat bacterial infection diseases such as urinary tract infections, sepsis and sexually transmitted infections have observed high resistance rates worldwide (WHO, 2021), and drugs like Amoxicillin, Norfloxacin, Metronidazole and Ciprofloxacin are associated with side effects and drug resistance further their effectiveness is reduced by long term use.

For more than 60 years, metronidazole (1) has served as an antibacterial and antiprotozoal agent. However, its prolonged usage has resulted in drug-resistance and associated with adverse effects. The use of metronidazole had been limited to anaerobic microorganism since their electron-transport system is sufficiently negative to reduce nitro group and activate their bactericidal effect. Metronidazole is usually not effective on facultative anaerobes from Gram-negative and Gram-positive such as *Staphylococcus aureus, Escherichia coli* and *Pseudomonas aeruginosa* (Jarrad *et al*., 2015). However most life-threatening pathogens are facultative anaerobes due to their ability to grow in the presence or in the absence of oxygen and are thus well-adapted to these changing conditions (André *et al*, 2021).

Nowadays there are reports of metronidazole analogues with potent activity against the facultative anaerobic bacteria indicate that there is a different mode of action of metronidazole (Jarrad *et al*., 2015). As a result, it is important to synthesize new metronidazole analogs with unique mode of action in order to enhance the antibacterial efficacy of metronidazole while reducing toxicity.

1.3 Objectives of the study

3.1.2.1 General objective

To synthesis and evaluate the *in vitro* anti-bacterial activity and target binding capability of 1-(2-ethyl acetate)-2-styryl metronidazole derivatives.

3.1.2.1 Specific objectives

- To synthesize, purify and characterize 1-(2-ethyl acetate)-2-styryl and 2-styryl metronidazole derivatives
- To evaluate *in vitro* anti-bacterial activity of 1-(2-ethyl acetate)-2-styryl and 2-styryl metronidazole derivatives on various bacterial strains.

- To conduct *In silco* study of 1-(2-ethyl acetate)-2-styryl and 2-styryl metronidazole derivatives

1.4 Significance of the study

Recent studies have shown that the enzyme FabH (β-ketoacyl-acyl carrier protein synthase III), responsible for the first step of fatty acid biosynthesis (FAB), is a promising target for nitroimidazole derivatives that can be used as an effective anti-infective. Fatty acid biosynthesis (FAB) is essential for the growth and viability of microorganisms. Consequently, Bacterial fatty acid synthase (FAS) is a prospective target for novel drug development.

A study has shown that acetyl-CoA is the preferred substrate at active site Cys 112 (Qiu *et al*., 2001). We hypothesize that incorporating acetyl groups in the synthesized compounds may result in substrate specificity at the binding site and exert a biological effect. Thus, this study aimed at exploring the synthesis of 1-(2-ethyl acetate)-2-styryl and 2-styryl metronidazole derivatives with modifications made at position one using ethyl acetate moiety. Findings from this study, which include evaluation of antibacterial activity and molecular docking study of the synthesized compounds, expected to provide a baseline for further optimization and design of potent FabH inhibitor drug molecule.

2 Literature Review

2.1 Nitroimidazole drugs as anti-infectives

Nitroimidazoles are a class of organic compounds that contain a nitro group and an imidazole heterocyclic ring. They have shown diverse biological properties such as anticancer, antifungal, antiprotozoal, antiviral, antibacterial and anti-TB activities. They are usually considered as structural alerts due to the fact that drugs containing nitro groups can induce severe toxicity. However, selective toxicity of nitroaromatic and heteroaromatic compounds makes them significant scaffolds for developing drugs against bacteria, parasites, or tumor cells without harming the host organism or normal cells (Nepali *et al*., 2019).

The emergence of nitroimidazoles reported in 1950s, when azomycin was isolated from a crude extract of *Streptomyces* bacteria (Ang *et al*., 2017). azomycin exhibited potent activity against *Trichomonas vaginalis*. Synthesis of 5-nitroimidazole regioisomer of azomycin lead to the discovery of Metronidazole with greater activity as an antiprotozoal drug for the treatment of trichomoniasis and amoebiasis, caused by *Trichomonas vaginalis, Entamoeba histolytica, Giardia lamblia.* Metronidazole was later found to be effective against anaerobic bacteria such as the Gram-negative *Bacteroides fragilis* (which causes peritoneal infections), the Gram-positive *Clostridium difficile* (which causes pseudomembranous colitis), and *Helicobacter pylori* (which causes stomach ulcers) (Mukherjee & Boshoff, 2011). It is now extensively used for treating infections caused by these organisms.

In the 1960s and 1970s, a second generation of 5-nitroimidazoles, including tinidazole, ornidazole, and secnidazole, was created. These compounds have similar broad-spectrum activity but were more effective than metronidazole. (Ang *et al*., 2017). Dimetridazole, a metronidazole counterpart with a methyl group instead of a

hydroxyethyl group at the 1-position, was similarly found to have antiprotozoal action. It was primarily used to treat parasite illnesses in livestock, such as histomoniasis and trichomoniasis, but it was banned by the European Commission due to its possible carcinogenicity in humans (Ang *et al*., 2017). At the same time, new nitroimidazoles with promising anti-trypanosome activity were identified. Megazol and fexinidazole were among the nitroimidazoles. Megazol was found to have promising efficacy against *Trypanosoma brucei* and *Trypanosoma cruzi*, as well as modest activity against *Leishmania donovani* Unfortunately, megazol development was halted due to mutagenic and genotoxic effects discovered in vitro and in vivo (Ang *et al*., 2017).

Metronidazole first shown antitubercular effectiveness against anaerobic, nonreplicating Mycobacterium tuberculosis in the mid-1990s (Ang *et al*., 2017). There was no activity against aerobic, actively replicating M. tuberculosis, highlighting its efficacy against anaerobic pathogens (Mukherjee & Boshoff, 2011).

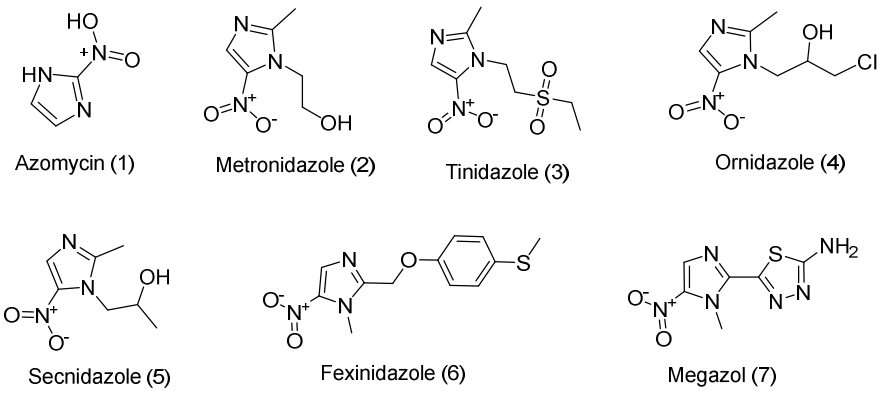

Figure 1: First and second generation of nitroimidazoles

2-Nitroimidazoles synthesized in the 1970s have been shown to have antitubercular activity. However, they possess reduction potentials that are approximately 150 mV higher than those of 5-nitroimidazoles and are therefore more readily reduced by

mammalian cells relative to 5-nitroimidazoles, resulting in nonselective side effects (Mukherjee & Boshoff, 2011; Ang *et al*., 2017).

Because of this unfavorable feature, research in the nitroimidazole scaffold for anti-infectives has been concentrated on the 4- and 5-nitroimidazole regioisomers. However, 2-nitroimidazoles have found use as radiosensitizers in cancer treatment, increasing tumor cell sensitivity to radiation therapy (Ang *et al*., 2017).

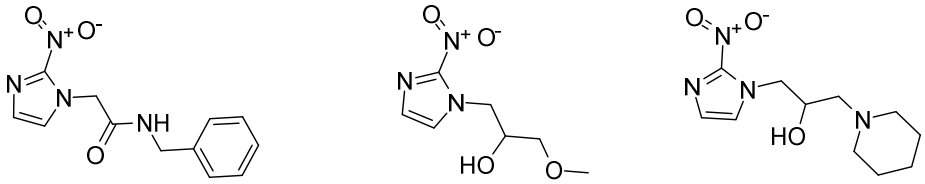

Figure 2: 2-Nitroimidazoles

CGI-17341, discovered by Hindustan Ciba-Geigy in 1989, was the first bicyclic nitroimidazole found to have *in vitro* and *in vivo* antitubercular action. Despite the fact that the chemical was efficient against drug-resistant TB and multidrug-resistant bacteria, further development was terminated due to mutagenicity reported in the Ames test. The scaffold's promising antitubercular action prompted further improvement and creation of related chemicals. After more than a decade of research, two novel bicyclic nitroimidazoles, delamanid (OPC-67683) and pretomanid (PA-824), were discovered to be mutagenic (Ang *et al*., 2017).

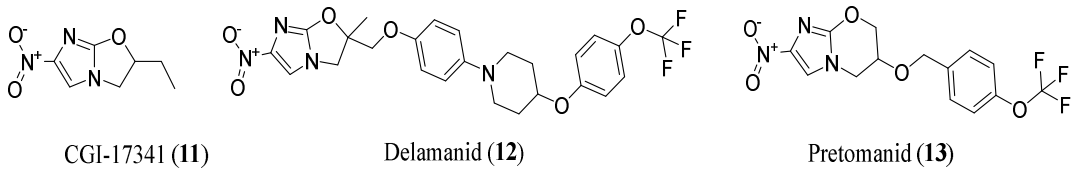

Figure 3: Bicyclic Nitroimidazoles

2.2 Mechanism of action of nitroimidazoles

Nitroimidazoles are considered as pro-drugs that the nitro group can be bioactivated by enzymatic reduction to give reactive species. These reactive species are responsible for the biological effects of nitro drugs; in this case the nitroaromatic compound is acting as a pro-drug (Patterson & Wyllie, 2014; Ang *et al*., 2017). While the nitro group is important for the pharmacological action, variations in the imidazole substituents result in various pharmacokinetic properties.

Although the exact molecular mechanisms of nitroimidazoles are difficult to decipher, the mechanism is generally assumed to involve two steps: first, reductive bioactivation of the nitro group, resulting in the generation of radicals and other reactive intermediates, and then the radicals and reactive intermediates react with cellular components such as DNA or protein (Ang *et al*., 2017; Gupta *et al*., 2022).

The therapeutic and cytotoxic effects of nitro compounds are induced through enzymatic reduction, usually by nitroreductases (NTRs) using prosthetic groups such as flavin mononucleotide (FMN) or flavin adenine dinucleotide (FAD), and reducing agents such as nicotinamide adenine dinucleotide (NADH) or nicotinamide adenine dinucleotide phosphate (NADPH) (Nepali l. *et al*, 2019). The bioactivation of nitro groups through enzymatic reduction varies depending on the reduction potential and conditions of the target organism (Gupta *et al*., 2022). Reduction can occur through a one- or two- electron mechanism. Under anaerobic conditions, the redox potential of the electron-transport system in microbes is sufficiently negative to reduce sequential two-electron generates amines via nitroso and hydroxylamine intermediates (Patterson & Wyllie, 2014). When nitroso and hydroxylamine react with biomolecules, they can have toxic and mutagenic effects. Hydroxylamines can also be transformed into reactive nitrenium ions, which can bind to DNA. Only one-electron reduction happens

in the presence of oxygen, resulting in the creation of a nitro radical anion that is unstable and promptly reoxidized by molecular oxygen back to the parent drug nitro group. This process, known as the "futile cycle," reduces bactericidal activity and is responsible for the harmful effects of nitro compounds by producing a reactive superoxide anion (Patterson & Wyllie, 2014; Ang *et al*., 2017).

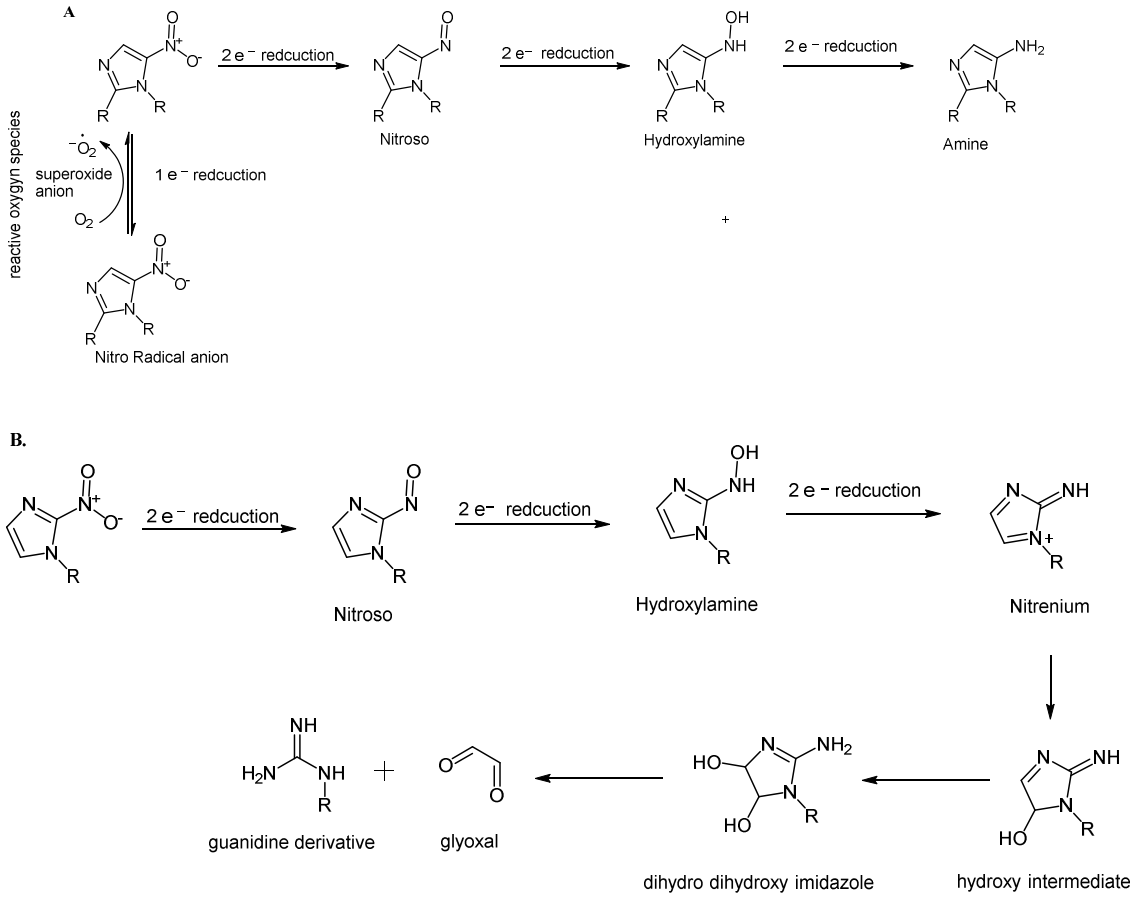

Figure 4: Mechanism of nitroreductase (NTR) catalysed bioactivation of nitroimidazoles. A. NTR-catalyzed reductions of 5-nitroimidazoles. B. NTR-catalyzed reductions of 2-nitroimidazoles.

2.3 β-ketoacyl-acyl carrier protein synthase III (FabH)

Recent study has identified the fatty acid synthesis (FAS) pathway in bacteria as a prospective target, and fatty acid biosynthesis (FAB) is a crucial metabolic activity for microorganisms that is required for cell viability and growth. The synthesis of fatty

acids in bacteria is conducted by type II bacterial fatty acid synthases (FAS) which are different from the synthases found in eukaryotes (mammals and fungi; type I) which are large multifunctional proteins. Whereas type II FAS system of plants, procaryotes and protozoa consists of many discrete monofunctional enzymes involved in condensation, reduction and dehydration (Zhang *et al*., 2012)

In most bacteria, -Ketoacyl-acyl carrier protein synthase III (FabH) catalyzes the first stage of fatty acid production via a type II fatty acid synthase. FabH proteins from Gram-positive and Gram-negative bacteria are substantially conserved in sequence and structure, whereas humans have no significantly comparable proteins. FabH catalyzes the condensation of acetyl-CoA with malonyl-ACP (acyl carrier protein) to create -ketoacyl-ACP, the first step in the fatty acid synthesis cycle. During this process, long-chain fatty acids are generated, which are required for cell membrane integrity and energy storage (Nie *et al*., 2005).

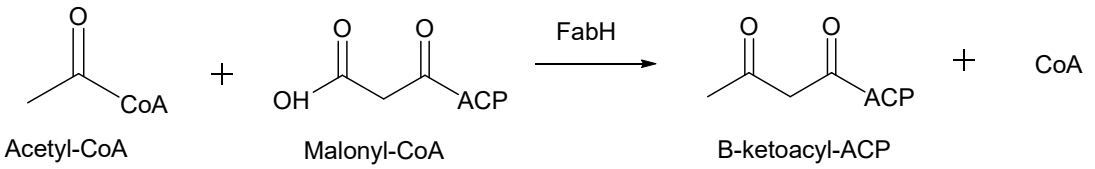

Figure 5: FabH-catalyzed initiation reaction of fatty acid

The crystal structure of FabH has been resolved, revealed that it contains an active site essentially invariant in various bacterial FabH molecules among members of the β-ketoacyl-ACP synthase family. The enzyme has a catalytic triad consisting of residues Cys112, His 244, and Asn 274 which are responsible for the catalytic activity of the enzyme(Qiu *et al*., 2001). Study on crystal structure of *E. coli* FabH complexed with various ligand provided evidence that acetyl-CoA (**Error! Reference source not found.**) was the preferred substrate at active site Cys 112 (Qiu *et al*., 2001).

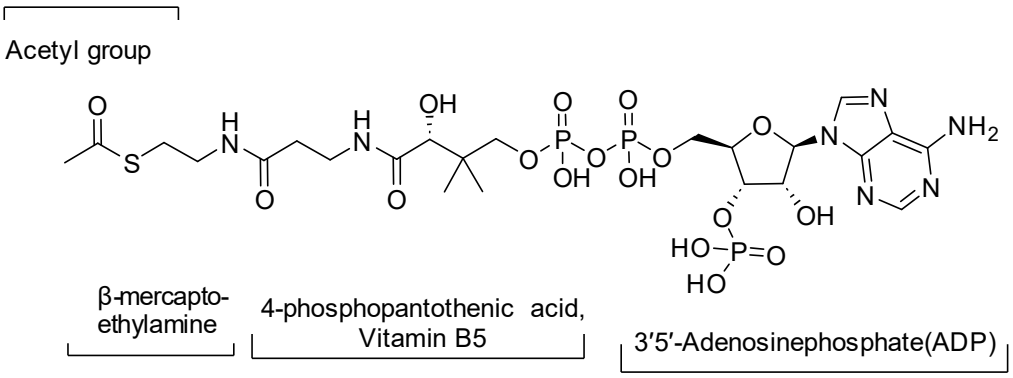

Figure 6: Structural formula of Acetyl-CoA and its constituents

The active cite Cys 112 provides essential thiol group in the enzymatic reaction of condensation. Four conserved basic residues (Arg 36, Arg 151, Lys 214, and Arg 249) and two conserved aromatic residues (Trp 32 and Phe 213) flank the entrance to the active cite. This makes the surface mixed hydrophobic and electropositive character. Conserved hydrophobic residues line the inner surface of the tunnel. Three completely conserved residues Cys112, His 244, and Asn 274) lie at the bottom of the tunnel (Qiu *et al*., 2001; Zhang *et al*., 2012)

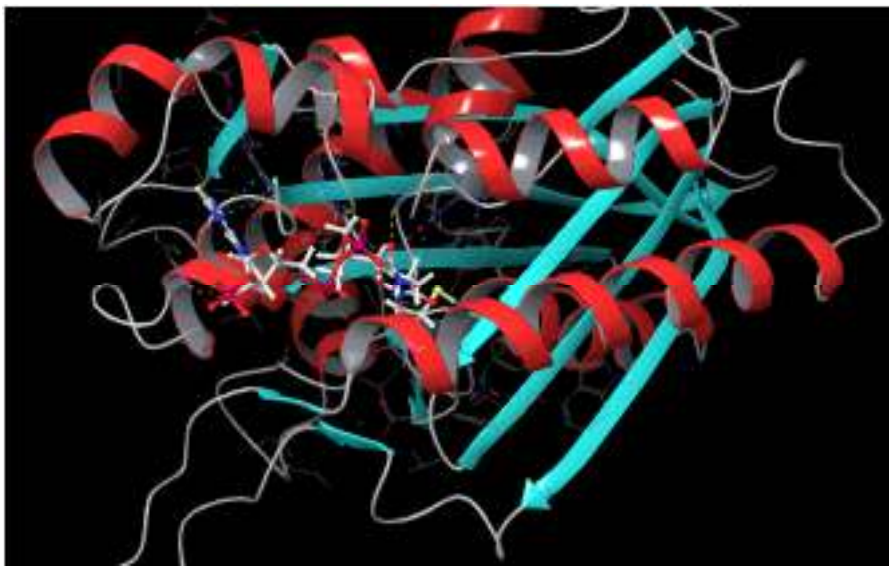

Figure 7: The CoA binding in the secondary structure of FabH

Because it regulates and controls the rate of fatty acid production in an initiating route, FabH has emerged as a promising target for the development of novel antimicrobial medicines, and its substrate selectivity plays a vital role in membrane fatty acid composition. These findings imply that small molecule inhibitors of FabH enzymatic activity could be used to generate selective, safe, and broad-spectrum antibacterials (Li *et al*., 2009; Zhang *et al*., 2011; Zhang *et al*., 2011).

2.4 Nitroimidazoles as inhibitors of β-ketoacyl-acyl carrier protein synthase III (FabH)

Novel compounds that inhibit FabH found in Gram-positive and Gram-negative bacteria, including multi-drug resistant strains, have been identified. Nitroimidazoles have been increasingly studied for their potential as antimicrobial agents. One area of interest for the use of nitroimidazoles is their ability to inhibit the function of β-ketoacyl-acyl carrier protein synthase III (FabH).

Previous research has shown that nitroimidazole derivatives exhibit antibacterial capabilities, lending credence to the notion that FabH can be employed as an effective molecular target for nitroimidazole derivatives (Wang *et al*., 2013; Zhang *et al*; Li *et al*; 2013; Qin *et al*., 2014; Duan *et al*., 2014; Zhang *et al*., 2014). FabH inhibitory activity of 2-styryl 5-nitroimidazoles also explored based on by previous studies 2-position modified 5-nitroimidazole drugs can overcome metronidazole resistance (Li *et al*., 2013;Wang *et al*; 2013; Duan *et al*., 2014;)

In 2013, Li *et al*. and his colleagues synthesized and investigated the structure-activity correlation of a novel class of secnidazole derivatives with Schiff base, as well as their antibacterial properties on *Pseudomonas aeruginosa*, *Escherichia coli*, and *Staphylococcus aureus, Bacillus subtilis* as well as *E. coli* FabH inhibitory activities. (Li *et al*., 2013) Among all compounds examined, a molecule with a trimethyl

substitution displayed potent efficacy against all strains, with MICs ranging from 3.13-6.25 g/mL versus Kanamycin (MICs = 1.56-3.13 g/mL). The same molecule has the highest *E. coli* FabH inhibitory activity (IC50 = 2.3 M) compared to other compounds.

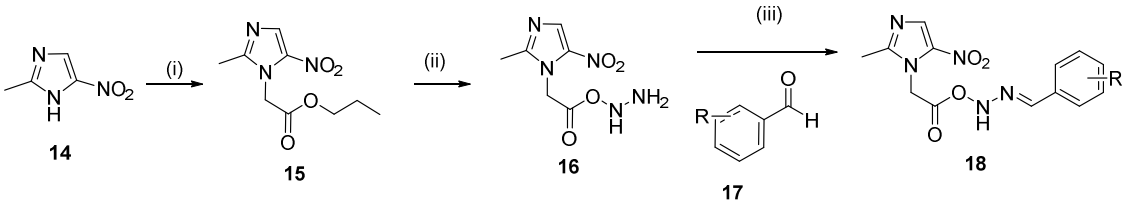

Reagents and conditions: (i) $ClCH_2CO_2Et$, K_2CO_3, acetone; (ii) hydrazine. hydrate, MeOH, reflux;(iii) MeOH, reflux.

Figure 8: Synthesis of 2-(2-methyl-5-nitro-1H-imidazol-1- yl) derivatives

Qin *et al*. (2014) published the synthesis of metronidazole-thiazole conjugates in 2014. Using kanamycin as a positive reference, a series of ten novel compounds (**25/26**) were synthesized and tested for antibacterial properties towards Gram-negative bacteria (E. *coli and P. aeruginosa*) and Gram-positive bacteria (*B. subtilis and B. thuringiensis*). Compounds (**25a-d** and **26a-b**) shown superior antibacterial properties against tested microorganisms when compared to kanamycin. MTT results revealed that compounds **25a-b** had the most powerful activity against *P. aeruginosa, B. subtilis, and B. thuringiensis,* with IC50 values ranging from 1.9 to 5.9 g/mL. In terms of inhibitory activity against E. Coli FabH, 25a was more powerful than the positive control kanamycin, with an IC50 value of 26.9 g/mL. Furthermore, **25a** and **25b** had the highest inhibitory efficacy against E. coli FabH, with IC50s of 4.9 and 5.2 M, respectively, when compared to kanamycin (IC50 of 6.8 M) (Qin *et al*., 2014).

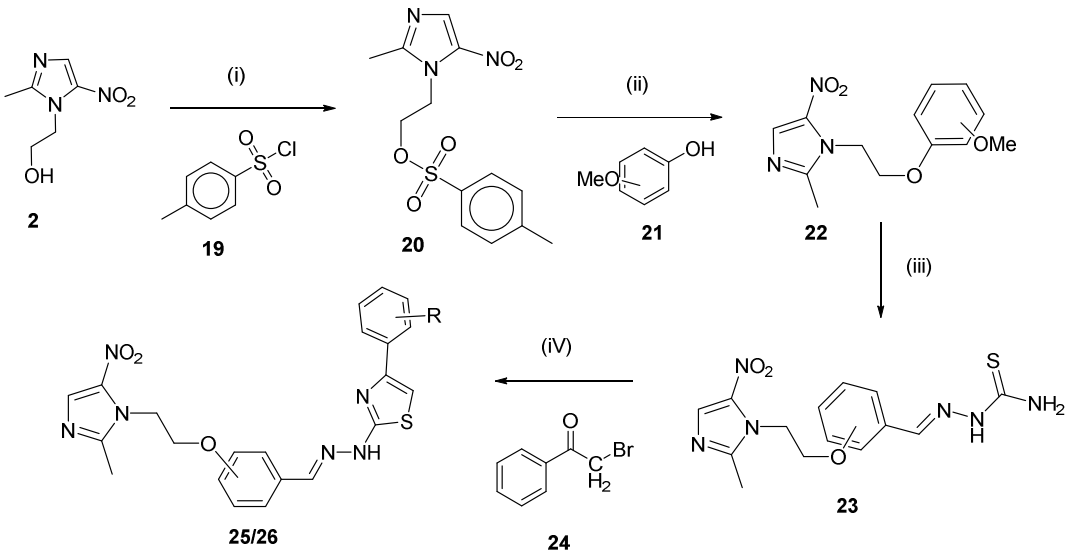

Compounds **25** para position **25** meta position **25a** R = *o*-Br, **25b** R = H, **25c** R = *p*-OMe, **25d** R = *p*-CF3 **26a** R = *p*-OMe, **26b** R = *p*-CF3

Reagents and conditions: (i) CH_2Cl_2, rt, 12 h (ii) K_2CO_3, DMF, 80 °C, 20 h (iii) $NH_2(CS_2)$, $NHNH_2$, isopropanol, CH_3COOH, 24 h (iv) isopropanol, rt, 48 h

Figure 9: Synthesis of metronidazole-thiazole derivatives

In 2014, Duan *et al*. reported the synthesis of 2-styryl derivatives of metronidazole utilizing aryl aldehydes. The antibacterial properties of newly created substances against *E. coli, P. aeruginosa, B. subtilis,* and *B. thuringiensis* strains revealed that compounds para-F and OMe derivatives demonstrated comparable inhibitory activity against P. aeruginosa with IC50 values 1.7-6.8 g/mL than kanamycin (6.8 g/mL) and penicillamine (5.8 g/mL). Benzyloxy at para position displayed greater efficacy against E. coli than kanamycin (47.3 g/mL) and penicillamine (42.3 g/mL), with IC50 values of 36.4 and 34.3 g/mL, respectively. The inhibiting efficacy of active compounds against *E. coli* FabH and *P. aeruginosa* FabH revealed that para NO_2 and Benzyloxy are the most potent inhibitors, with IC50 values of 2.1 and 3.4 M (against *E. coli* FabH) and 7.9 and 10.2 M (against *P. aeruginosa* FabH), respectively, comparable to

kanamycin (3.1 and 6.7 M). Compounds containing para NO_2 and Benzyloxy have computed docking energies of -35.54 and -33.17 kcal/mol, indicating that the compounds are possible FabH inhibitors.

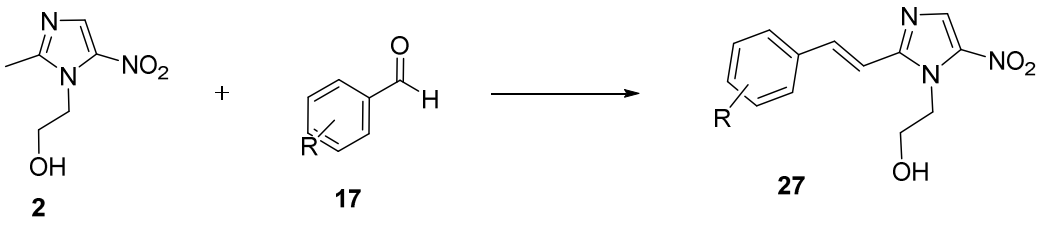

Reagents and conditions: (i) NaOMe, DMSO, methanol, rt.

Figure 10: Synthesis of metronidazole-styryl derivatives

Li *et al*. (2014) reported the synthesis of novel metronidazole-Schiff's base derivatives in 2014. Using kanamycin B and penicillin G as positive controls, all **29/30** produced compounds were tested for antibacterial properties on Gram-negative bacteria (*E. coli* ATCC 35218 and *P. aeruginosa* ATCC 13525) and Gram-positive bacteria (B. subtilis ATCC 6633 and *S. aureus* ATCC 6538). Compound **29a** was discovered to be the most effective and to have a wide range of effects. When compared with the positive control kanamycin B (0.78-3.13 g/mL) and penicillin G (1.56-6.25 g/mL), the spectrum of efficacy against all tested strains had IC50 values in the range of 1.56-3.13 g/mL. Compounds having para sulfonamide (-SO2NH-), para methoxy, and para methyl groups inhibited *E. coli* FabH the most effectively, with IC50 values of 2.6883, 5.5923, and 4.928 M, respectively, as compared with secnidazole **5** (IC50 = 28.5 M) and Metronidzole (**2**) (IC50 = 17.6 M). The molecular docking investigation of active compounds in the active site of E. coli FabH revealed that the molecule with (-SO2NH-) substitution had the lowest binding energy of -55.3117 kcal/mol and was stabilized to the FabH kinase through H-bond and - interactions.

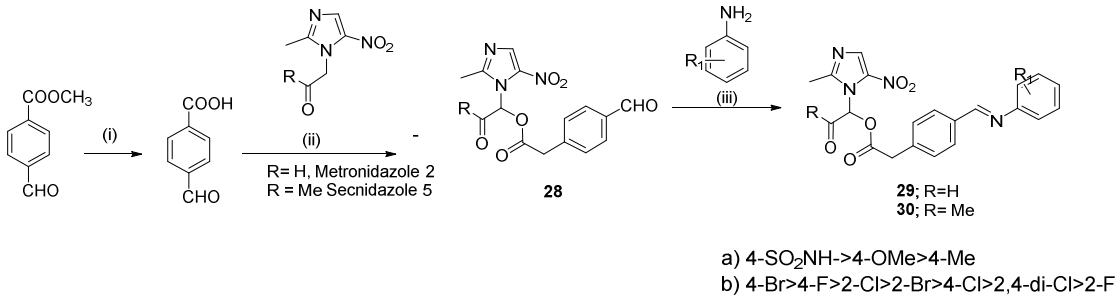

Reagents and conditions: (i) MeOH: H_2O (1:1), 2M NaOH, rt, 4 h; (ii) EDC.HCl, DMAP, DCM, reflux, overnight; (iii) EtOH, reflux, overnight

Figure 11: Synthesis of metronidazole/Secnidazole-Schiff's bases

3 MATERIALS AND METHODS

3.1 Materials

3.1.1 Chemicals and reagents

The chemicals used include 4-(dimethylamino) benzaldehyde 99% (BDH, England), 2-Methyl-5-nitroimidazole-1-ethanol 98%, benzaldehyde 99% obtained from Department of Chemistry, Faculty of Science, Addis Ababa University, acetic anhydride, dimethyl sulfoxide (DMSO), hexane, ethyl acetate, dichloromethane, methanol, chloroform (from BDH and Sigma-Aldrich Co., MO, USA) were used for the synthesis, purification and chromatogram of the compounds. All the solvents were of analytical grade.

3.1.2 Instruments

Silica gel analytical TLC plates (60 F254, 0.2 mm thick, Merck KGaA, Darmstadt, Germany) and column silica gel (60 F254, 70 - 240 mesh, Merck KGaA, Darmstadt, Germany) were used for the analysis and purification for the compounds during synthesis. Rotary evaporator (BUCHI Rotavapor™ R-300, Switzerland) was used for the removal of solvents.

Incubator (Modell 100-800 memmert), autoclave, biosafety cabinet (biostar modell50/60), vortex (Fisher Brand), water bath, inoculating loops, electrical weighing balance, magnetic stirrer, cavate, test tube, pipette tips, pipette filler, micro-pipette (10-200µl), micro-titter plates, capillary tube and measuring cylinder were used for synthesis and antimicrobial test.

UV-Visible Spectrophotometer (Evlution 60S) was used to visualize the TLC chromatogram plates. NMR spectra were recorded using 400 MHz for 1H and 100 MHz for ^{13}C on a Bruker Avance DMX400 FT-NMR spectrometer (Bruker, Billerica,

Massachusetts, USA), tetramethyl silane (TMS) as internal standard and $CDCl_3$ was used as solvent.

3.1.3 Media, microbial strains and standard drugs

Nutrient Agar (NA), Mueller-Hinton Broth (MHB), Sabouraud Dextrose Agar (SDA) and Sabouraud Dextrose Broth (SDB) (HiMedia Laboratories Pvt. Ltd. India), (Sisco Research Laboratories Pvt. Ltd. India) were used for the media preparation.

Ciprofloxacillin a positive control for antibacterial test, was obtained from Ethiopian Public Health Institute (EPHI). The gram-positive bacterial strains *Staphylococcus aureus* (ATCC 25923), *Staphylococcus epidermidus* (ATCC 281214) and *Streptococcus agalactiae* (ATCC 12386) and the gram-negative bacterial strains *Escherichia coli* (ATCC 25922), *Pseudomonas aeruginosa* (ATCC 27853) and Klebsiella *pneumoniae* (ATCC 700603) were used as *in vitro* antibacterial test organisms. The microorganisms were obtained from Ethiopian Public Health Institute (EPHI)

3.2 Methods

3.2.1 Synthesis

2-styryl metronidazole derivatives were synthesized as described by Duan *et al,* (2014) through a reaction of metronidazole with various substituted benzaldehyde in DMSO by rapidly adding a stirred solution containing sodium methoxide in methanol under room temperature. (Figure 12). Further acetylation of the products to produce 1-(2-ethyl acetate)-2-styryl 5-nitroimidazole derivatives are obtained as described by (Anbu *et al*., 2019) solvent free and catalytic free condition. 1 mmol of substrate (2-styryl metronidazole) mixed homogeneously 1.5 mmol acetic anhydride using a glass rod, and then placed in a warmed oil bath kept at 60°C overnight. The refined compounds were obtained by subsequent purification with column chromatography. The products of the

synthesis were recrystallized from proper solvents and characterized by ^{1}H and ^{13}C NMR spectrometry. based on available published data compound **33** and compound **36** are synthesized for the first time.

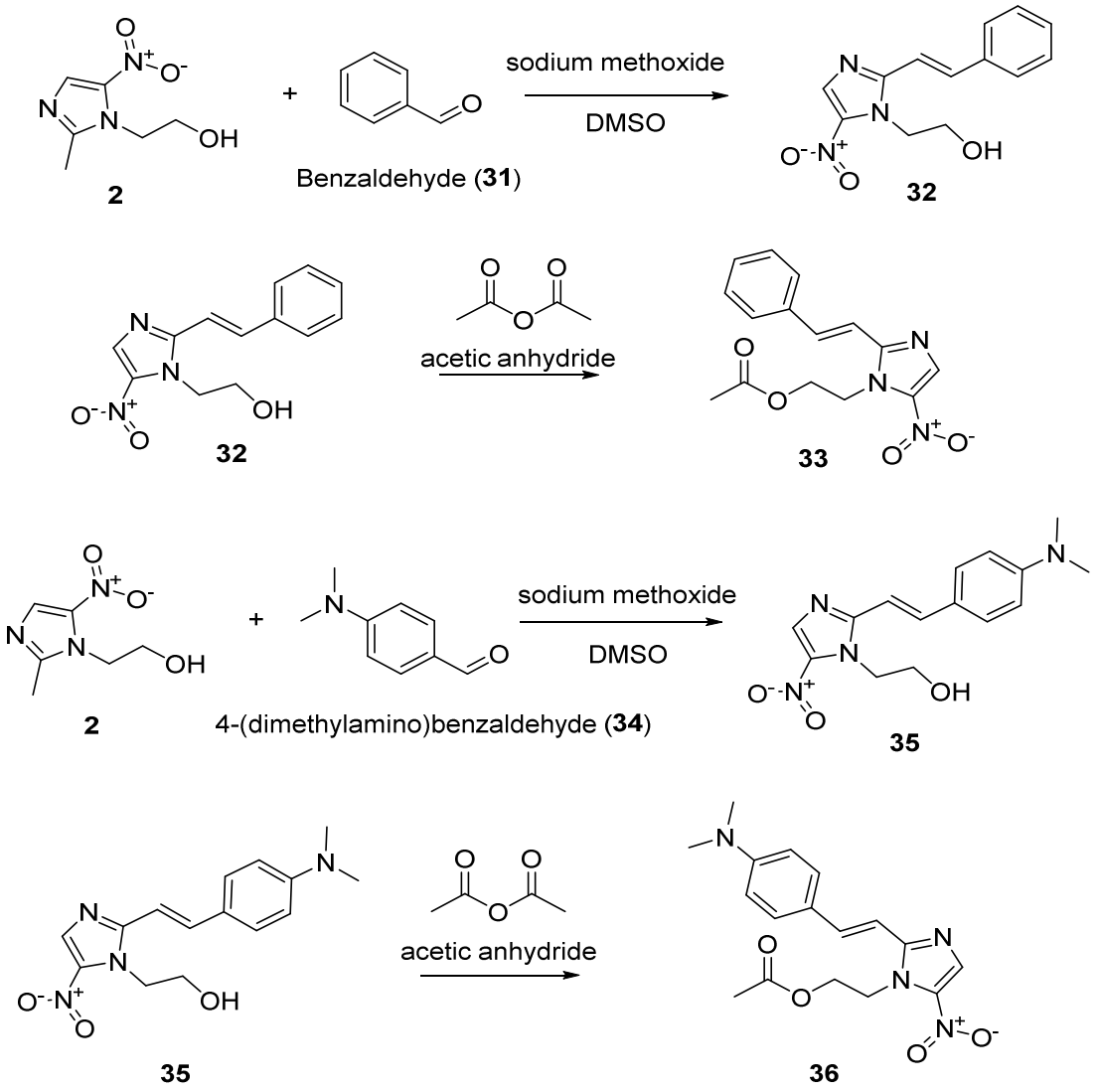

Figure 12: Chemical structures of synthesized 3-styryl-5-nitrometronidazole derivatives

(*E*)-2-(5-nitro-2-styryl-1H-imidazol-1-yl)ethan-1-ol (32)

Compounds 32 was prepared from 2.05 g (12 mmol) of metronidazole with benzaldehyde 1.77ml (16 mmol) in 6 ml of DMSO by adding rapidly a stirred

solution of 1.3 g (12.8 mmol) sodium methoxide in methanol. The completion of the reaction was monitored diluted with diethyl ether by analytical TLC using Chloroform: Ethyl acetate (3:2) as a mobile phase. when the reaction completed the mixture was extracted three times with diethyl ether, dried over anhydrous sodium sulfate, dried in vacuum and purified by silica gel column chromatography with increasing gradient of Ethyl acetate in Chloroform as eluting solvent.

(*E*)-2-(5-nitro-2-styryl-1H-imidazol-1-yl)ethyl acetate (33)

Compounds **33** was prepared from 1 g (3.86 mmol) of Compounds **32** followed by the addition of 0.546 ml (5.78 mmol) acetic anhydride. This mixture was homogeneously mixed with the help of a glass rod and later placed in a preheated water bath maintained at 60^0C overnight. The reaction's completion was monitored solubilizing with diethyl ether by analytical TLC using Chloroform: Ethyl acetate (3:2) as a mobile phase. when the reaction completed the mixture was extracted three times with diethyl ether, dried over anhydrous sodium sulfate and dried in vacuum to give 2 (1.12 g, 96.55 %). The assigned structure was compatible with the spectrum data ^{1}H NMR and ^{13}C NMR.

(*E*)-2-(2-(4-(dimethylamino)styryl)-5-nitro-1H-imidazol-1-yl)ethan-1-ol (35)

Compounds **35** was prepared from 2.05 g (12 mmol) of metronidazole with benzaldehyde 1.77ml (16 mmol) in 6 ml of DMSO by adding rapidly a stirred solution of 2.4 g (12.8 mmol) sodium methoxide in methanol. The reaction mixture was allowed to stir overnight at room temperature. The completion of the reaction was monitored diluted with diethyl ether by analytical TLC using Chloroform: Ethyl acetate (3:2) as a mobile phase. when the reaction completed the mixture was extracted three times with diethyl ether, dried over anhydrous sodium sulfate, dried

in vacuum and purified by silica gel column chromatography with increasing gradient of Ethyl acetate in Chloroform as eluting solvent to give 3 (1.65 g, 45.5%). The assigned structure was compatible with the spectrum data ^{1}H NMR and ^{13}C NMR.

(*E*)-2-(2-(4-(dimethylamino)styryl)-5-nitro-1H-imidazol-1-yl)ethylacetate (36)

Compounds **36** was prepared from 1 g (3.31 mmol) of Compounds **35** followed by the addition of 0.450 ml (4.96 mmol) acetic anhydride. This mixture was homogeneously mixed with the help of a glass rod and later placed in a preheated water bath maintained at $60^{0}C$ overnight. The reaction's completion was monitored solubilizing with diethyl ether by analytical TLC using Chloroform: Ethyl acetate (3:2) as a mobile phase. when the reaction completed the mixture was extracted three times with diethyl ether, dried over anhydrous sodium sulfate and dried in vacuum to give 4 (1.1 g, 96.57 %). The assigned structure was compatible with the spectrum data ^{1}H NMR and ^{13}C NMR.

3.2.2 Antibacterial Activity Assay

3.2.2.1 Preparation of media, inoculum and standardization

All culture media used were prepared according to the manufacturer instruction. The media was sterilized at 121 ^{0}C for 15 minutes using an autoclave and allowed cool to 45 ^{0}C-50 ^{0}C in water bath. Then 20 ml of media was poured into 100 mm diameter size petri-dishes under aseptic condition inside level II Bio-safety Cabinet (Bioair instruments, Eurolone Company, Italy) and allowed some time to solidify. All the selected strains were sub-cultured on Petri dishes containing nutrient agar media. The antimicrobial experiment was conducted according to Eloff and the Clinical and Laboratory Standards Institute (CLSI) guideline. For antimicrobial experiments 4-5

bacterial colony for each tested organisms were inoculated with inoculating loop in to Petri dishes containing agar medium. Each bacterial test organisms were incubated for 18-24 h at 37 °C and up to 7 days at 25°C, respectively. Standardization was accomplished by preparing a suspension of 3-5 inoculations from a fresh, pure culture of the specimen bacterium in Mueller Hinton broth. The produced suspension's absorbance was measured using an ultraviolet-visible (UV) spectrophotometer (Thermo Scientific Evolution 60s CAT 840210100) at 625 nm having a path length of 1cm until the absorbance reading was 0.08 to 0.1, which is proportional to $1x10^8$ colony forming unit (CFU)/mL bacteria. The standardized solution was then further diluted with Muller Hinton Broth at a 1:100 ratio to yield a colony suspension containing 1 $x10^6$ CFU/mL bacteria. For the broth dilutions, final suspensions of 5 $x10^5$ CFU/mL were employed, and they were employed to evaluate the antibacterial activity of the compounds in comparison to both positive and negative controls (Eloff, 1998).

3.2.2.2 Minimum inhibitory concentration determination

Microtiter broth dilution method was performed on synthesized compounds. The Minimum inhibitory concentration (MIC) of the synthesized compounds was determined according to (Eloff, 1998) and the Clinical and Laboratory Standards Institute (CLSI) guidelines (CLSI, 2015) . Stock solutions, a concentration of 1 mg/ml, of the respective compounds were prepared by dissolving in 5% DMSO and distilled water. A 100µl of Muller Hinton broth was added into each well of the 96-well microplates. From a stock solution, the serial dilutions were made ranging from 100 µg/ mL to 0.0156 µg/mL using Mueller–Hinton broth in 96-well microplates. The bacterial suspension containing approximately 5×10^5 colony-forming units/ml was prepared from a refreshed culture. From this suspension, 100 µl was inoculated into each well and incubated for18-24 hours at 37 °C. After incubation, 40 µl of a 0.4 mg/ml

solution of MTT [3-(4,5-dimethylthiazol-2-yl)-2,5-diphenyltetrazolium bromide was added to each well as an indicator of microbial growth and incubated at 37 °C for 30 minutes. After incubation, the MIC values were visually determined by observing the presence or absence of purple color. The MIC was determined as the lowest concentration of every well that produced no apparent purple color. The MIC values were calculated in triplicate. For each strain, a sterility control well and a growth control well were also investigated. Positive control procedures with ciprofloxacin at a starting dose of 10µg/ml in sterile water were carried out in parallel to assess the sensitivity of the bacteria. A negative control trial with only 5% DMSO was also carried out.

3.2.3 *In silico* studies

3.2.3.1 In Silico Prediction of ADMET property.

Qikprop of Maestro v11.5 was utilized to assess the absorption, distribution, metabolism, and excretion (ADME) prediction of synthesized compounds.

3.2.3.2 Molecular docking study

Molecular docking of the synthesized compounds was performed on the E. coli FabH-CoA complex structure downloaded from the PDB (1HNJ.pdb) (www.rcsb.org). Molecular modelling studies was carried out using the Schrödinger suite 2023 version 1 (Schrödinger Inc., New York, USA).

The protein preparation wizard module of the Schrödinger suite was utilized for preparing the protein by adding hydrogens, correcting errors such as absent side chains, allocating appropriate bond ordering, and altering ionization and tautomeric states (through epik). All water molecules have been eliminated. All atoms will be optimized and then minimized with OPLS3 force fields, with the come together heavy atoms to RMSD set to 0.3 (default). Preparation of Ligands Compounds drawn in ChemDraw

SD format were imported and prepared using the Ligprep module, which performed hydrogen addition, 2D to 3D conversion, ionization and tautomeric state generation (via Epik) at the physiological pH 7.0 2.0, and also produced ring configurations via the standard settings.

Induced Fit Methodology was used to dock compounds to 1HNJ using Schrödinger. In conventional virtual docking experiments, the binding site of a receptor is docked with ligands where the receptor is maintained rigid and the ligand is allowed to move. However, as many proteins in reality experience side-chain or backbone movements, or both, upon ligand binding, the assumption of a rigid receptor can lead to misleading conclusions. These changes enable the receptor to alter its binding site so that it better conforms to the shape and binding mode of the ligand. In the case that the receptor considerably adjusts to the presence of the ligand, Induced Fit Docking (IFD) technique aims to enhance the docking of ligands (Elekofehinti *et al*., 2021; Sherman *et al*., 2006).

3.2.4 Statistical analysis

IBM SPSS (Statistical Package for Social Sciences) Statistics for Windows, Version 20.0, was used to analyze the data. IBM Corp., Armonk, New York. The results were presented as mean standard deviation of mean (M SD). To compare antimicrobial activity assay values between treatment and control groups, statistical significance was established using one-way ANOVA followed by the Tukey post hoc test where at $P<0.05$, the result was declared statistically significant.

4 RESULTS AND DISCUSSIONS

For more than 60 years, metronidazole (1) has served as an antibacterial and antiprotozoal agent. However, its prolonged usage has resulted in drug-resistance and associated with adverse effects. Furthermore metronidazole (1) is usually not effective on Gram-negative and Gram-positive facultative anaerobic bacteria, which are considered as the most life-threatening pathogens. However, there are reports of metronidazole analogues with potent activity against the facultative anaerobic bacteria indicate that there is a different mode of action of metronidazole. As a result, it is important to synthesize new metronidazole analogs with unique modes of action in order to enhance the antibacterial efficacy of metronidazole while reducing toxicity.

4.1 Synthesis of compounds

In this study, we synthesized 2-styryl metronidazole derivatives through a condensation reaction between metronidazole and benzaldehyde, facilitated by sodium methoxide. This reaction is a Knoevenagel type reaction, a modified Aldol Condensation reaction that forms C-C bonds via a nucleophilic addition between an aldehyde or ketone and an active hydrogen compound in the presence of a basic catalyst. The 2-methyl group of 2-methyl-5-nitroimidazoles contain acidic protons (stabilized by the neighboring C=N), which can be abstracted by sodium methoxide to form a strong nucleophile that attacks the carbonyl carbon of the aldehyde, followed by the loss of water molecule, resulting in the formation of the target compound **32** as depicted in Figure **13**.

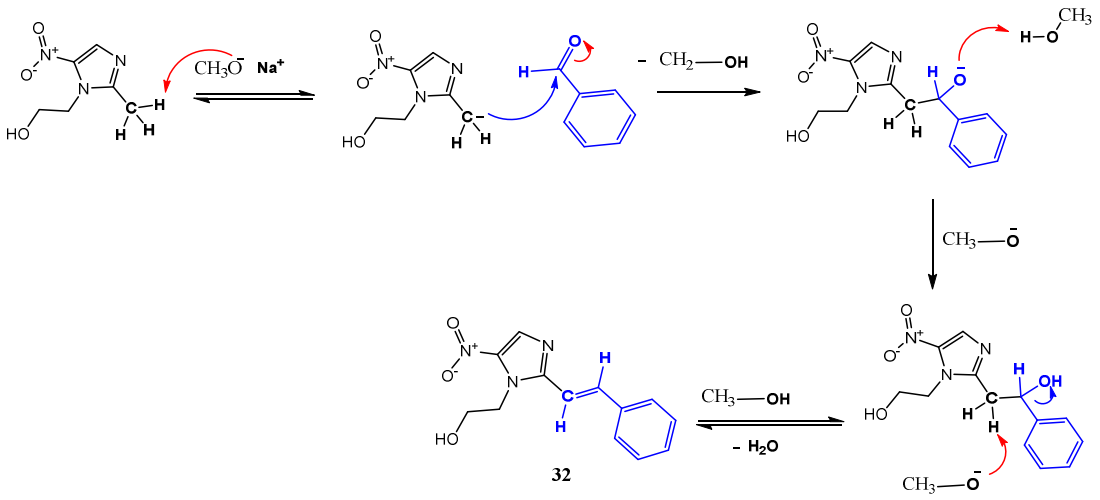

Figure 13: Proposed mechanism of action of condensation reaction

While acetylation using acyl halide or acid anhydride by catalysis of acids or bases, metal salts, and metal nanoparticles is well known for its advantages such as low reaction temperature, higher yield, and fast reaction time, has limitations in work-up and purification process. In our situation, we followed a straightforward and effective procedure proposed by Anbu and his coworkers (Anbu *et al*., 2019) for the acetylation of 2-styryl metronidazole utilizing acetic anhydride under solvent and catalyst free conditions. According to (Anbu *et al*., 2019), this technique offers good selectivity and full conversion under moderate reaction temperature and air atmosphere.

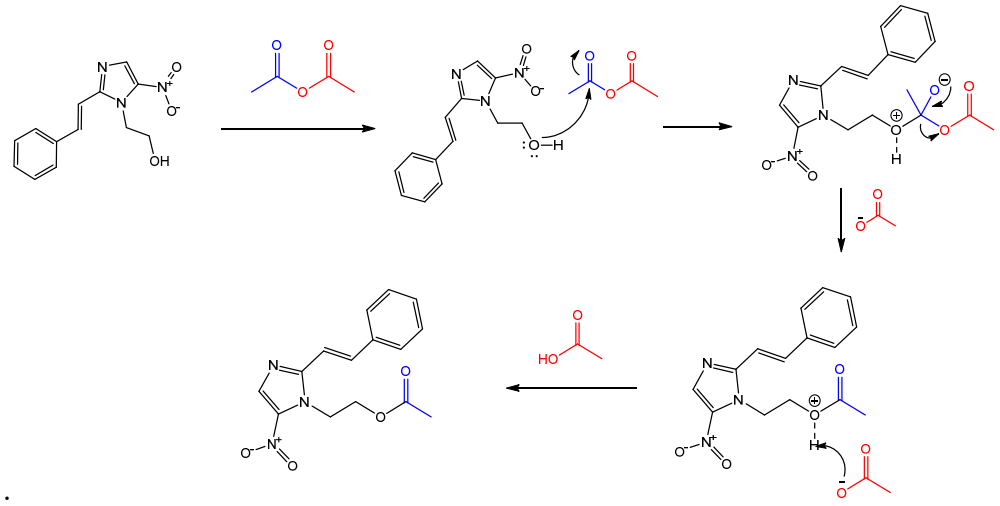

.

Figure 14: Proposed mechanism of action of acetylation reaction

4.2 Structural elucidation of synthesized compounds

(*E*) 2-(5-nitro-2-styryl-1H-imidazol-1-yl)ethan-1-ol (32)

Compound **32** was obtained as yellow solid (2.36 g, 76%). ^{1}H NMR (DMSO-d6, 400 MHz) δ: 8.25 (s, 1H, CH), 7.80 (1H, CH), 7.48-7.65 (m, 2H, ArH), 7.36-7.45 (m, 4H, ArH, CH), 5.045 (s, 1H, OH), 4.61 (t, 2H, CH_2), 3.72 (q, 2H, CH_2). Presence of 8 Hs downfield chemical shifts ranging from 7.36 – 7.80 and the coupling pattern J= ~ 6.8 supports the presence of aromatic moiety with an ortho coupling. Further the coupling pattern J=15.6 confirms the presence of methylene moiety with trans configuration. The most up-field singlet with δ: 8.25 is in agreement with the presence of proton in the imidazole ring. The broad and shorter peak at 5.045 which integrate to 1H revealed the presence of OH moiety. The two triplet and quartet upfield signals δ_H:4.61 and 3.72 which integrate to 4Hs revealed the presence of two 2Hs (N-CH_2, O-CH_2), deshielded due to the electronegativity of the oxygen and the electron withdrawing effect of the nitrogen of imidazole ring. This was also consistent with DEPT spectrum of two negative signals at δ_C: 47.85 and δ_C: 60.58.

(*E*)-2-(5-nitro-2-styryl-1H-imidazol-1-yl)ethyl acetate (33)

Compounds **33** was obtained as yellow solid (1.12 g, 96.55 %). ^{1}H NMR (DMSO-d6, 400 MHz) δ: 8.25 (s, 1H, CH), 7.83 (1H, CH), 7.78-7.79 (m, 2H, ArH), 7.39-7.47 (m, 4H, ArH, CH), 4.87 (t, 2H, CH_2), 4.39 (t, 2H, CH_2), 1.8 (s, 3H, CH_3). Presence of 8 Hs downfield chemical shifts ranging from δ_H 7.39 – 7.83 and the coupling pattern J= ~ 6.8 supports the presence of aromatic moiety with an ortho coupling. Further the coupling pattern J=15.6 confirms the presence of methylene moiety with trans configuration. The most up-field singlet with δ_H: 8.25 is in agreement with the presence of proton in the imidazole ring. The two upfield signals with triplet and quartet splitting

patten which integrate to 4Hs reveals the presence of two 2Hs (N-CH_2, O-CH_2). deshielded due to the electronegativity of the oxygen and the electron withdrawing effect of the nitrogen imidazole ring. This was also consistent with DEPT spectrum of two negative signals at δ_C: 47.85 and δ_C: 60.58. ^{13}C NMR chemical shift δ_C: 170.3 confirmed that the presence of ester carbonyl.

(*E*)-2-(2-(4-(dimethylamino)styryl)-5-nitro-1H-imidazol-1-yl)ethan-1-ol (35)

Compounds **35** was obtained as orange solid (1.65 g, 45.5%). ^1H NMR (DMSO-d6, 400 MHz) δ: 8.25 (d, 1H, CH), 8.20 (s, J=11.7MHz, 1H, CH), 7.57 (d, 2H, ArH), 7.07 (d, J=11.7MHz, 1H, CH), 6.72 (m, 2H, ArH), 5.01 (s, 1H, OH), 4.56 (t, 2H, CH_2), 3.71 (q, 2H, CH_2) 2.95 (s, 6H, CH_3).

Presence of 7 Hs chemical shifts ranging from δ_H 6.71 – 7.71 dwnfield and the coupling pattern J= ~ 6.8 supports the presence of aromatic moiety with an ortho coupling. Further the coupling pattern J=15.6 confirms the presence of methylene moiety with trans configuration. The most up-field singlet with δ_H: 8.2 is in agreement with the presence of proton in the imidazole ring. The broad and shorter peak at 5.01 which integrate to 1H reveal the presence of OH moiety. The two triplet and quartet upfield signals δ_H:4.56 and 3.71 which integrate to 4Hs revealed the presence of two 2Hs (N-CH_2, O-CH_2), deshielded due to the electronegativity of the oxygen and the electron withdrawing effect of the nitrogen of imidazole ring. This was also consistent with DEPT spectrum of two negative signals at δ_C: 47.85 and δ_C: 60.58. Further integral of 6 Hs in one singlet peak at δ_H: 2.95 was evident the presence of two methyl groups attached to electronegative N atom.

(*E*)-2-(2-(4-(dimethylamino)styryl)-5-nitro-1H-imidazol-1-yl)ethyl acetate (36)

Compounds **36** was obtained as orange solid (1.1 g, 96.57 %). ^{1}H NMR (DMSO-d6, 400 MHz) δ_H: 8.2 (s, 1H, CH), 7.7 (d, J=11.7MHz, 1H, CH), 7.57 (d, 2H, ArH), 7.05 (d, J=11.7MHz, 1H, CH), 6.74 (m, 2H, ArH), 4.802 (t, 2H, CH_2), 4.37 (t, 2H, CH_2), 1.8 (s, 3H, CH_3).

Presence of 7 Hs chemical shifts ranging from δ_H 6.72 – 7.71 downfield and the coupling pattern J= ~ 6.8 supports the presence of aromatic moiety with an ortho coupling. Further the coupling pattern J=15.6 confirms the presence of methylene moiety with trans configuration. The most up-field singlet with δ_H: 8.2 is in agreement with the presence of proton in the imidazole ring. The two triplet upfield signals δ_H:4.802 and 4.37 which integrate to 4Hs reveals the presence of two 2Hs (N-CH_2, O-CH_2), deshielded due to the electronegativity of the oxygen and the electron withdrawing effect of the nitrogen of imidazole ring. This was also consistent with DEPT spectrum of two negative signals at δ_C: 47.85 and δ_C: 60.58. Further integral of 6 Hs in one singlet peak at δ_H: 3.00 was evident the presence of two methyl groups attached to electronegative N atom. ^{13}C NMR chemical shift δ_C:170.36 confirmed that the presence of easter carbonyl.

Table 1: ^{1}H and ^{13}C NMR data synthesized compound

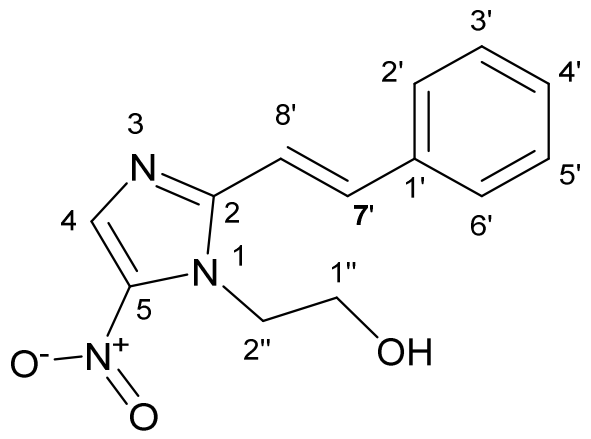

Compound **32**

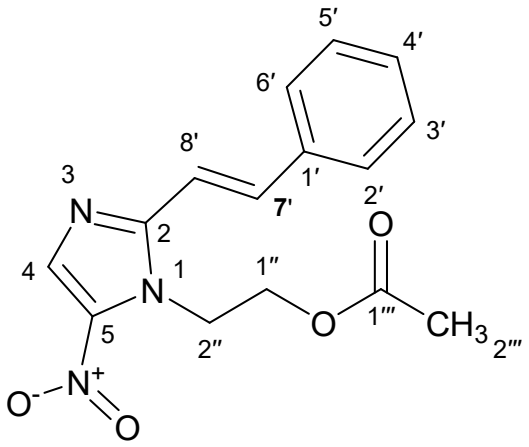

Compound **33**

Position	**δC (ppm)**	**δH (ppm)**	**Position**	**δC (ppm)**	**δH (ppm)**
1″-(O-CH_2)	60.57	3.72 (2H, *m*, CH_2)	2‴-(CO$\underline{C}H_3$)	20.8	1.80 (3H, *s*, CH_3)
2″- (N-CH_2)	47.85	4.61 (2H, *t,* CH_2)	1‴ -($\underline{C}OCH_3$)	170.30	
1″		5.04 (1H, *s,* OH)	1″ -(O-CH_2)	62.74	4.39 (2H, *t* CH_2)
8′,3′,4′,5′	114.42, 128.12, 129.82	7.36-7.45 (4H, *m,* ArH, CH)	2″ -(N-CH_2)	44.42	4.87 (2H, *t,* CH_2)
2’,6’	129.28	7.48-7.65 (J=8.5, 2H, *m,* ArH),	8′,3′,4′,5′	113.72, 128.16, 129.35	7.39-7.46 (4H, ArH, *m,* CH)
7′	138.05	7.803 (1H, CH)	2’,6’	129.98	7.78-7.79 (2H, *m,* ArH),
4	135.20	8.25 (1H, *s,* CH)	7′	139.14	7.83 (1H, CH)
1′	136.20		4	135.90	8.25 (1H, *s,* CH)
5	139.15		1′	135.32	
2	151.05		5	138.59	
			2	150.79	

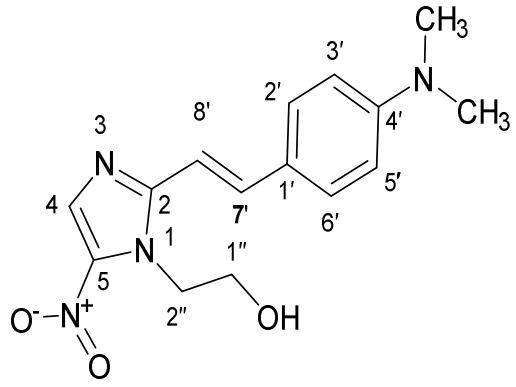

Compound **35**

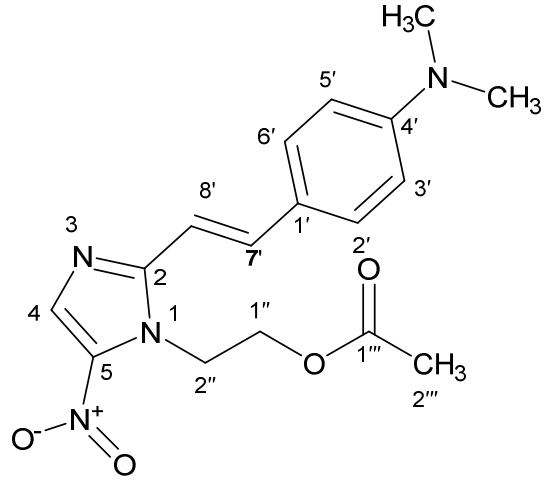

Compound **36**

Position	**δC (ppm)**	**δH (ppm)**	**Position**	**δC (ppm)**	**δH (ppm)**
4′-N(CH_3)$_2$	40.21	2.95 (6H, *s,* CH_3)	4′-N(CH_3)$_2$	40.21	3.00 (s, 6H, CH_3)
1″ -(O-CH_2)	60.59	3.71 (2H, *m,* CH_2)	1‴-($COCH_3$)	20.84	1.80 (s, 3H, CH_3)
2″ - (N-CH_2)	47.62	4.56 (2H, *t,* CH_2)	2‴-($COCH_3$)	170.36	
1″		5.01 (1H, *s,* OH)	1″-(O-CH_2)	62.75	4.37 (t, 2H, CH_2)
3′,5′	108.52	6.72 (2H, *m,* ArH)	1″-(N-CH_2)	44.19	4.80 (t, 2H, CH_2)
8′	112.3	7.06 (1H, *d,* CH),	3′,5′	107.75	6.74 (m, 2H, ArH)
2’,6’	129.64	7.57 (2H, *d,* ArH)	8′	112.34	7.05 (d, 1H, CH),
7′	135.75	7.70 (1H, *d,* CH)	2’,6’	129.71	7.57 (2H, *d,* ArH)
4	139.22	8.20 (1H, *s,* CH)	7′	135.92	7.70 (1H, *d,* CH)
1′	123.62		4	139.7	8.20 (1H, *s,* CH)
5	138.78		1′	123.46	
2	151.55		5	138.71	
4′	152.42		2	151.67	
			4′	152.23	

4.3 Antimicrobial activities of synthesized compounds

The synthesized compounds were tested *in vitro* antibacterial activity against six bacterial strains, including three Gram-positive (*S. aurius, S. agalactiae, S. faecalis*) and three Gram-negative (*E. coli and P. aeruginosa and K. pneumonia*) strains, using the MTT method. Interestingly, all compounds demonstrated significant activity

against all tested bacterial strains, with an MIC value ranged 1.56 µg/mL -41.67 µg/mL, as indicated in Table 1. Of all tested bacterial strains,

Further examination of the findings for Gram-positive bacteria, compound **33** and **36** had similar activity against *S.aurius* compared to compound **32** and **35.** However, these two compounds had a significantly better performance against *S.agalactiae* with MIC value 1.56 µg/mL. *S.agalactiae* is main source of invasive bacterial disease in neonatal, including meningitis due to its ability to pass blood–brain barrier (BBB) and invade the central nervous system(Nagao, 2015). Compound **36** showcased the maximum activity against the other Gram-positive strain *S.faecalis* with an MIC value of 1.56 µg/mL.followed by compound **33** with MIC value of 3.125 µg/mL. respectively.

With regards to Gram-negative bacteria compound **33** was the most potent against *E. coli* (MIC= 2.08 µg/mL), which is the most common cause of acute urinary tract infections as well as urinary tract sepsis. *Escherichia coli* also known to cause severe foodborne disease (Percival & Williams, 2014). Several countries also reported bloodstream infections caused by *E. coli* strain resistant to third generation cephalosporins (WHO, 2021). It is interesting to note that *Klebsiella pneumoniae* was the most vulnerable bacterial strain to both compounds **33** and **36**, with an MIC value of 6.25 µg/mL and 12.5 µg/mL, respectively. *K. pneumoniae* is a common gut bacterium that can cause potentially fatal infections. *K. pneumoniae* resistance to last-resort treatment (carbapenem antibiotics) has reported throughout the world (WHO, 2021). Both compound **33** and **36** had significantly potent activity against *P.aeruginosa* with MIC value 3.12 µg/mL. Pseudomonas aeruginosa cause of wound and mucosal surface infections in immunocompromised patients. It can cause burn wound infections, urinary tract infections, folliculitis, and is the predominant respiratory tract pathogen (Wu & Li, 2015). *P. aeruginosa* is a multidrug resistant pathogen where carbapenem-

resistant strain is included among WHO list of bacteria for which new antibiotics are urgently needed at critical status (WHO, 2017). However, *K. pneumonia* was found to be equally the least susceptible to both compounds **32** and **35**, with an MIC value of 25 µg/mL. *E. coli*, a bacterium that causes various infectious diseases, was the least susceptible to compound **35**, with an MIC value of 41.67 µg/mL.

These findings give insight compound **33** and **36** can be a candidate lead compound targeting Gram-positive bacteria which are invasive to blood–brain barrier (BBB) particularly *S.agalactiae.* Similarly compound **33** and **36** can be a good candidate lead compound for Gram-negative pathogens with widespread resistance have been developed such as *K. pneumoniae, E.coli* and *P.aeruginosa*

Table 2: Antibacterial activity of synthesized compounds

Compound type	MIC (µg/ml)						Average
	Gram-positive bacteria			Gram-negative bacteria			
	S.aurius	S.agalactiae	S.faecalis	E.coli	P.aeruginosa	K.pneumonia	
Compound **32**	12.5±0	12.5±0	6.25±0	12.5±0	12.5±0	25±0	13.54±1.36
Compound **33**	12.5±0	1.56±0	3.125±0	2.082±0.52	3.125±0	6.25±0	4.774±0.92
Compound **35**	10.42±2.08	12.5±0	12.5±0	41.67±8.33	12.5±0	25±0	19.10+2.97
Compound **36**	6.25±0	1.56±0	1.56±0	12.5±0	3.125±0	12.5±0	6.25±1.14
Ciprofloxacin	0.313±0	0.625±0	0.625±0	0.02±0	0.02±0	0.08±0	0.28±0.06

From Table 1, it was observed that acylated compounds **33** and **36** showed significantly higher activity against both Gram-positive and Gram-negative strains compared to compounds **32** and **35**. This may be attributed to incorporation of acetyl groups, as we have proposed. Additionally, non-substituted phenyl ring compounds **32** and **33** demonstrated better activity than the 4-aminodimetyl substituted phenyl ring compounds **35** and **36,** which is consistent with findings from previous studies (Wang *et al*., 2013). Thus, the presence of electron-donating substituents on the benzene ring,

such as 4-dimethylamino group, did not improve the antibacterial activity (Wang *et al*., 2013). However, this contrasts with other studies that have found (Duan *et al*., 2014) that substitutions at the phenyl ring led to more potent inhibitory activity against *E. coli* g (Duan *et al*., 2014).

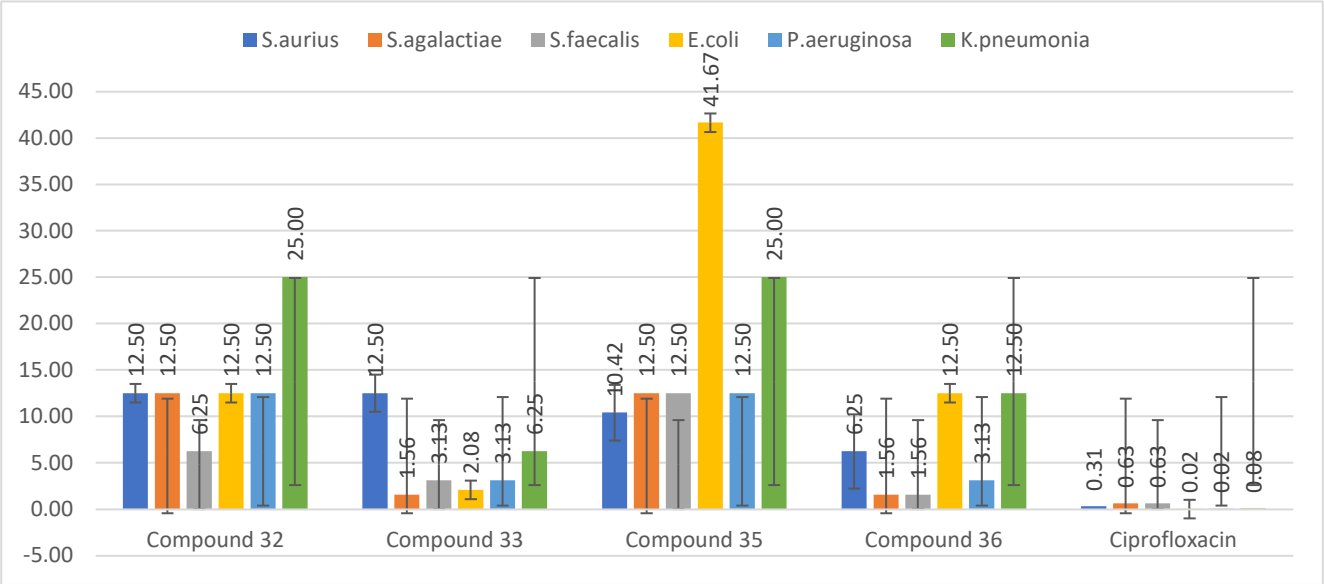

Figure 15: MIC value of tested compounds and the standard drug ciprofloxacin

4.4 In silico studies

4.4..1 In Silico Prediction of ADMET property

Table 1 displays the physicochemical and pharmacokinetics properties of synthesized compounds, as predicted by Qikprop. Analysis of the pharmacokinetic properties included predication of binding to human serum albumin (QPlogKhsa), total solvent accessible surface area (SASA), brain/blood partition coefficient (QPlogBB), Caco-2 cell permeability in nm/sec (QPPCaco), as well as the number of hydrogen bond donors and acceptors. All compounds fell within the recommended range, except for the IC_{50} value for the blockage of HERG K+ channels (QPlogHERG), which was found to be below -5 for all compounds. Table 2 shows the ADME prediction, wherein acylated

compounds **33** and **36** demonstrated enhanced lipophilicity, as evidenced by their QPlogPo/w values.

Table 3: ADME prediction Synthesized Compounds

Molecule	SASA[1]	donorHB[2]	accptHB3	QPlogPo/w[4]	QPlogS[5]	QPlogHERG[6]
Compound **32**	512.981	1	4.2	2.104	-3.016	-5.288
Compound **33**	552.021	0	4.5	2.582	-3.182	-5.027
Compound **35**	586.634	1	5.2	2.608	-3.793	-5.281
Compound **36**	689.139	0	5.5	3.292	-5.088	-6.036

QPPCaco[7]	QPlogBB[8]	QPlogKp[9]	QPlogKhsa[10]	HumanOral[11] Absorption	PercentHuman[12] OralAbsorption	RuleOfFive/[13] Three
297.882	-1.342	-2.832	-0.15	3	83.545	0
274.76	-1.346	-2.991	-0.07	3	85.718	0
398.04	-1.358	-2.776	-0.002	3	88.747	0
224.471	-1.818	-3.247	0.211	3	88.304	0

Property or Descriptors and range or recommended values

[1]SASA Total solvent accessible surface area (SASA) in square angstroms using a probe with a 1.4 Å radius 300.0 – 1000.0

[2]donorHB Estimated number of hydrogen bonds that would be donated 0.0 – 6.0

[3]accptHB Estimated number of hydrogen bonds that would be accepted 2.0 – 20.0

[4]QPlogPo/w Predicted octanol/water partition coefficient. −2.0 – 6.5

[5]QPlogS Predicted aqueous solubility, −6.5 – 0.5

[6]QPlogHERG Predicted IC50 value for blockage of HERG K+ channels. concern below −5

[7]QPPCaco Predicted apparent Caco-2 cell permeability in nm/sec. Caco-2 cells are a model for the gut-blood barrier <25 poor, >500 great

[8]QPlogBB Predicted brain/blood partition coefficient for orally delivered drugs −3.0 – 1.2

[9]QPlogKp Predicted skin permeability, log Kp. −8.0 – −1.0

[10]QPlogKhsa Prediction of binding to human serum albumin. −1.5 – 1.5

[11]HumanOralAbsorption Predicted qualitative human oral absorption: 1, 2, or 3 for low, medium, or high

[12]PercentHumanOralAbsorption Predicted human oral absorption on 0 to 100% scale. >80% is high <25% is poor

[13]RuleOfFive Number of violations of Lipinski's rule of five. The rules are: mol_MW < 500, QPlogPo/w < 5, donorHB ≤ 5, accptHB ≤ 10. Compounds that satisfy these rules are considered drug-like. (The "five" refers to the limits, which are multiples of 5.) maximum is 4

[13]RuleOfThree Number of violations of Jorgensen's rule of three. The three rules are: QPlogS > -5.7, QP PCaco > 22 nm/s, # Primary Metabolites < 7. Compounds with fewer (and preferably no) violations of these rules are more likely to be orally available. maximum is 3

4.4..2 Molecular docking study

The synthesized compounds were subjected to molecular docking with the *E. coli* FabH-CoA complex structure, obtained from PDB (1HNJ.pdb) (www.rcsb.org) via induced fit docking (IFD). It was shown that a rigid receptor can produce incorrect docking scores because proteins undergo specific rotations (backbone or side-chain) when they attach to ligands. These structural alterations allow the receptor to adapt its binding site to ensure it better conformations to the shape and binding of the ligand. The IFD approach enables this through allowing the target receptor to modify its binding pocket to make it more compatible with the shape and binding mode of the ligand.

Results from the molecular docking study indicated that compound **33** exhibited the most favorable docking score of -8.221 kcal/mol, followed by compound **36** with a docking score of -7.921 kcal/mol. Figure 16 displays how compound **33** had more

favorable interactions with *E. coli* FabH, yielding IFD scores of -678.22 kcal/mol and -677.91 kcal/mol, respectively. Additionally, both compounds bound nicely into the active site of FabH via several π-π and electrostatic interactions involving amino acids THR28, TRP32, ARG151, GLY209, MET207 and oxygen and nitrogen atoms of -NO_2 group.

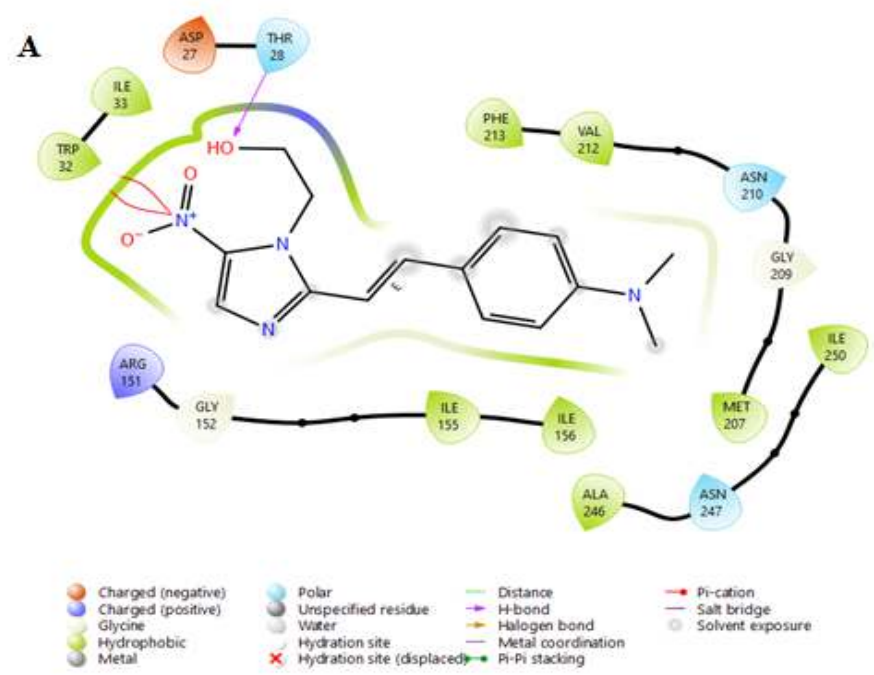

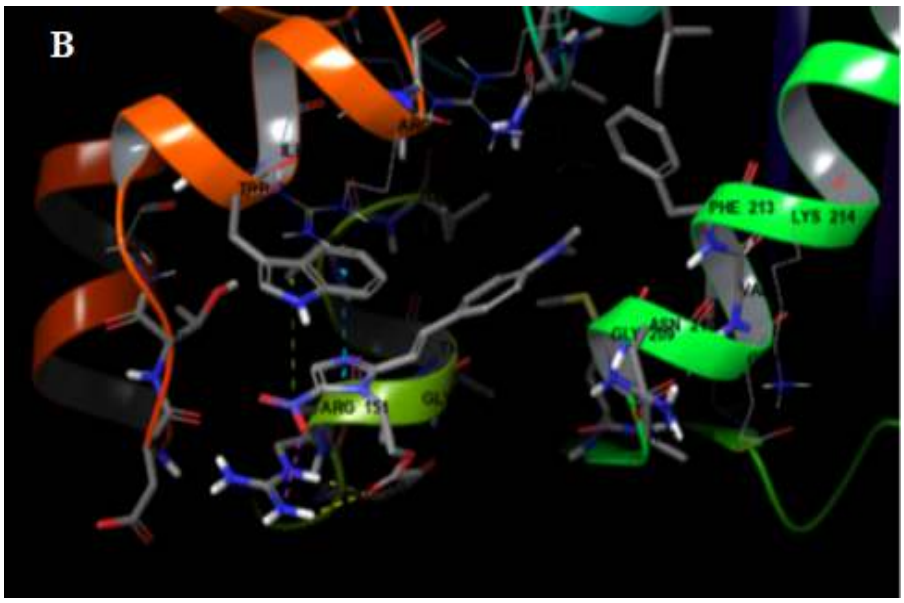

Figure 16: A. 2D interaction between compound 2 and E. coli FabH. B. 3D interaction between compound 2 and E. coli FabH'=

5 CONCLUSION AND RECOMMENDATION

We synthesized two derivatives of 5-metronidazole, 1-(2-ethyl acetate)-2-styryl and 2-styryl, and found that compounds **33** and **36** (1-(2-ethyl acetate)-2-styryl 5-metronidazole) demonstrated superior activity compared to compounds **32** and **35** (2-styryl 5-metronidazole). Compound **33** had a potential to be a lead compound to treat infectious disease caused by *E. coli* (MIC= 2.08 μg/mL) as it exhibited the most potent activity against E. *coli*, which is the leading cause of bacteria-mediated urinary tract infections, respiratory illness and pneumonia. *S. faecalis* was found to be the most susceptible bacterial strains to compound **36** (MIC= 1.56 μg/mL). Additionally, both compounds **33** and **36** equally showed the most substantial efficacy against *S. agalactiae*, *P. aeruginosa* and *K. pneumonia*.

Molecular docking studies against *E. coli* FabH-CoA complex structure (1HNJ.pdb) revealed that both compounds **33** and **36** displayed favorable hydrophobic and electrostatic interactions with conserved residues that line the inner surface into the active site.

Furthermore, we discovered that acetylation of 2-styryl -5-nitroimidazoles enhanced both their biological activity and binding interaction with the target protein. This improvement in activity was further supported by the predicted value of lipophilicity. We suggest further optimization of the lead compound by introducing a bulky or long alkyl group to the inner hydrophobic binding active site of the target protein. Additionally, we recommend to study the potential biological activity of the lead compounds against other pathogens that have a conserved β-ketoacyl-acyl carrier protein synthase III (FabH) protein structure, such as *Mycobacterium tuberculosis*.

6 REFERENCES

Anbu N, Nagarjun N, Jacob M, Vimala M, Kalaiarasi K, & Dhakshinamoorthy A (2019). Acetylation of alcohols, amines, phenols, thiols under catalyst and solvent-free conditions. *Chemistry*, **1**(1): 69-79

Ang W, Jarrad M, Cooper A, & Blaskovich T (2017). Nitroimidazoles: Molecular fireworks that combat a broad spectrum of infectious diseases. *Journal of Medicinal Chemistry*, **60**(18):7636–7657.

André AC, Debande L, Marteyn BS. (2021). The selective advantage of facultative anaerobes relies on their unique ability to cope with changing oxygen levels during infection. *Cell Microbiology*. **23**(8):e13338

Berhe D, Beyene G, Seyoum B, Gebre M, Haile K, Tsegaye M, Boltena M, Tesema E, Kibret T, Biru M, Siraj D, Shirley D, Howe R, & Abdissa, A (2021). Prevalence of antimicrobial resistance and its clinical implications in Ethiopia: a systematic review. *Antimicrobial Resistance and Infection Control* **10**(1): 168.

Christensen C, Kragelund B, Wettstein-Knowles P, & Henriksen A (2006). Structure of the human beta-ketoacyl [ACP] synthase from the mitochondrial type II fatty acid synthase. *Protein Science*, **16**(2): 261–272.

CLSI. (2015). M07-A10: Methods for dilution antimicrobial susceptibility tests for bacteria that grow aerobically*; Approved Standard—Tenth Edition*. www.clsi.org.

Duan Y, Wang Z, Sang Y, Tao X, Teraiya, S, Wang P, Wen Q, Zhou X, Ding L, Yang Y & Zhu H (2014). Design and synthesis of 2-styryl of 5-Nitroimidazole derivatives and antimicrobial activities as FabH inhibitors. *European Journal of Medicinal Chemistry*, **76:** 387–396.

Elekofehinti O, Iwaloye O, Josiah S, Lawal A, Akinjiyan M, & Ariyo E (2021). Molecular docking studies, molecular dynamics and ADME/tox reveal therapeutic potentials of STOCK1N-69160 against papain-like protease of SARS-CoV-2. *Molecular Diversity*, ***25***(3): 1761–1773.

Eloff, J. (1998). A sensitive and quick microplate method to determine the minimal inhibitory concentration of plant extracts for bacteria. *Planta Medica*, **64**(08): 711–713.

Gupta R, Sharma S, Singh R, Vishwakarma R, Mignani S, & Singh P (2022). Functionalized nitroimidazole scaffold construction and their pharmaceutical applications: A 1950–2021 comprehensive overview. *Pharmaceuticals* **15**(5):561

Ikuta K, Swetschinski L, Robles A, Sharara F, Mestrovic T, Gray A, Davis W, Wool E, Han C, Gershberg H, Aali A, Abate S, Abbasi-Kangevari M, Abbasi-Kangevari Z, Abd-Elsalam S, Abebe G, Abedi A, Abhari A, Abidi H,and Naghavi M (2022). Global mortality associated with 33 bacterial pathogens in 2019: a systematic analysis for the global burden of disease study 2019. *The Lancet*, **400**(10369): 2221–2248.

Jarrad A, Karoli T, Debnath A, Tay C, Huang J, Kaeslin G, Elliott A, Miyamoto Y, Ramu, S, Kavanagh A, Zuegg J, Eckmann L, Blaskovich M, & Cooper M (2015). Metronidazole-triazole conjugates: Activity against Clostridium difficile and parasites. *European Journal of Medicinal Chemistry*, *101*, 96–102. https://doi.org/10.1016/j.ejmech.2015.06.019

Li H, Shi L, Li Q, Liu P, Luo Y, Zhao J, & Zhu H (2009). Synthesis of C(7) modified chrysin derivatives designing to inhibit β-ketoacyl-acyl carrier protein synthase III (FabH) as antibiotics. *Bioorganic & Medicinal Chemistry*, **17**(17):6264–6269.

Li Y, Luo Y, Hu Y, Zhu D, Zhang S, Liu Z, Gong H, & Zhu H (2012). Design, synthesis and antimicrobial activities of nitroimidazole derivatives containing 1,3,4-oxadiazole scaffold as FabH inhibitors. *Bioorganic & Medicinal Chemistry*, **20**(14):4316–4322.

Li Y, Zhao C, Ma H, Zhao M, Xue Y, Wang X, & Zhu H (2013). Design, synthesis and antimicrobial activities evaluation of Schiff base derived from secnidazole derivatives as potential FabH inhibitors. *Bioorganic and Medicinal Chemistry*, **21**(11): 3120–3126.

Misganaw A, Naghavi M, Walker A, Mirkuzie A, Giref A, Berheto T, Waktola E, Kempen, J, Eticha G, Wolde T, Deguma D, Abate K, Abegaz K, Ahmed M, Akalu Y, Aklilu A, Alemu B, Asemahagn M, Awedew A, and Gebremedhin L (2022). Progress in health among regions of Ethiopia, 1990–2019: a subnational country analysis for the Global Burden of Disease Study 2019. *The Lancet*, **399**(10332):1322–1335.

Mukherjee T, & Boshoff H (2011). Nitroimidazoles for the treatment of TB: Past, present and future. In *Future Medicinal Chemistry* **3**(11):1427–1454).

Murray C, Ikuta K S, Sharara F, Swetschinski L, Robles A, Gray A, Han C, Bisignano C, Rao P, Wool E, Johnson S, Browne A, Chipeta M, Fell F, Hackett S, Haines-Woodhouse G, Kashef H, Kumaran E, McManigal B, and Naghavi M (2022). Global

burden of bacterial antimicrobial resistance in 2019: a systematic analysis. *The Lancet*, **399**(10325): 629–655.

Nagao P (2015). Streptococcus agalactiae (Group B Streptococci). Molecular Medical Microbiology 1751–1767). Elsevier.

Nepali K, Lee H, & Liou J (2019). Nitro-group-containing drugs. *Journal of Medicinal Chemistry* **62**(6):2851–2893.

Nie Z, Perretta C, Lu J, Su Y, Margosiak S, Gajiwala K, Cortez J, Nikulin V, Yager K, Appelt K, & Chu S (2005). Structure-based design, synthesis, and study of potent inhibitors of β-ketoacyl-acyl carrier protein synthase III as potential antimicrobial agents. *Journal of Medicinal Chemistry*, **48**(5):1596–1609.

Patterson S, & Wyllie S (2014). Nitro drugs for the treatment of trypanosomatid diseases: Past, present, and future prospects. In *Trends in Parasitology* **30(**6): 289–298).

Percival S, & Williams D (2014). Escherichia coli. *Microbiology of Waterborne Diseases* 89–117. Elsevier.

Qin Y, Wang P, Makawana J, Wang Z, Wang Z, Yan-Gu J & Zhu H (2014). Design, synthesis and biological evaluation of metronidazole-thiazole derivatives as antibacterial inhibitors. *Bioorganic and Medicinal Chemistry Letters*, **24**(22), 5279–5283.

Qiu X, Janson C, Smith W, Head M, Lonsdale J & Konstantinidis A (2001). Refined structures of β-ketoacyl-acyl carrier protein synthase III. *Journal of Molecular Biology*, **307**(1): 341–356.

Sherman W, Day T, Jacobson M, Friesner R, & Farid R (2006). Novel procedure for modeling ligand/receptor induced fit effects. *Journal of Medicinal Chemistry*, **49**(2): 534–553.

Wang Z, Duan Y, Qin Y., Wang P, Luo Y, Wen Q, Yang Y, Sun J, Hu Y, Sang Y & Zhu H (2013). Potentiating 1-(2-hydroxypropyl)-2-styryl-5-nitroimidazole derivatives against antibacterial agents: Design, synthesis and biology analysis. *European Journal of Medicinal Chemistry*, **65**: 456–463.

WHO. (2017, February 27). *WHO publishes list of bacteria for which new antibiotics are urgently needed*. https://www.who.int/news/item/27-02-2017-who-publishes-list-of-bacteria-for-which-new-antibiotics-are-urgently-needed

WHO. (2021, November 17). *Antimicrobial resistance*. Https://Www.Who.Int/News-Room/Fact-Sheets/Detail/Antimicrobial-Resistance.

Wu M, & Li X. (2015). Klebsiella pneumoniae and Pseudomonas aeruginosa. *Molecular Medical Microbiology* **3**: 1547–1564).

Zhang H, Li Z, & Zhu, H (2012). Advances in the Research of β-Ketoacyl-ACP Synthase III (FabH) Inhibitors. *Current Medicinal Chemistry*, **19**(8): 1225–1237.

Zhang H, Zhu D, Li Z, Sun J, & Zhu H (2011). Synthesis, molecular modeling and biological evaluation of β-ketoacyl-acyl carrier protein synthase III (FabH) as novel antibacterial agents. *Bioorganic and Medicinal Chemistry*, **19**(15):4513–4519.

Zhang H, Qin X, Liu K, Zhu D, Wang X, & Zhu H (2011). Synthesis, antibacterial activities and molecular docking studies of Schiff bases derived from N-(2/4-benzaldehyde-amino) phenyl-N′-phenyl-thiourea. *Bioorganic & Medicinal Chemistry*, **19**(18), 5708–5715.

Zhang X, Sangani C, Jia L, Gong P, Wang F, Wang J, & Zhu H (2014). Synthesis and antibacterial evaluation of novel Schiff's base derivatives of nitroimidazole nuclei as potent *E. coli* FabH inhibitors. *RSC Advances*, **4**(97):54217–54225.

7 APPENDICES

7.1 ^{1}H, ^{13}C and DEPT-135 NMR spectra of synthesized compounds

^{1}H, ^{13}C and DEPT-135 NMR spectra of Compound **32**

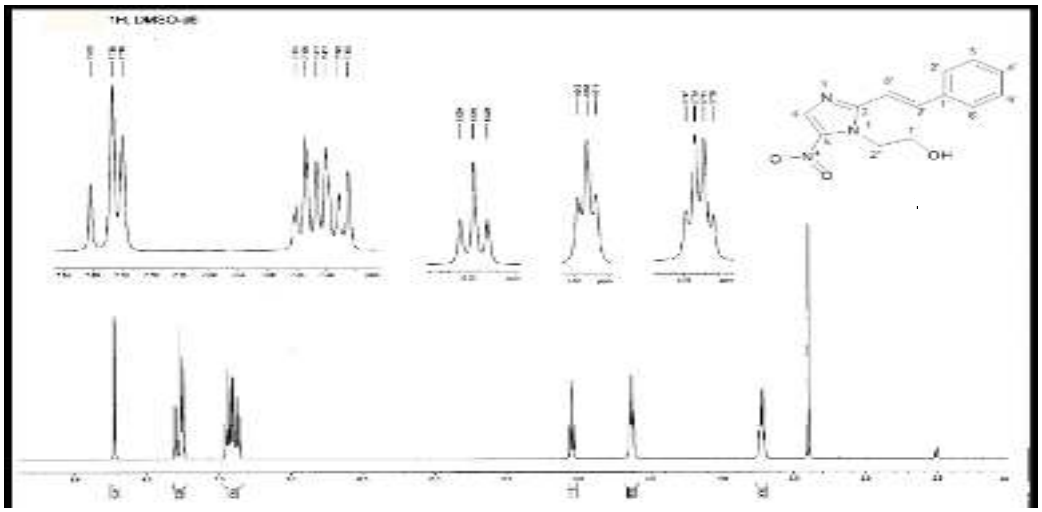

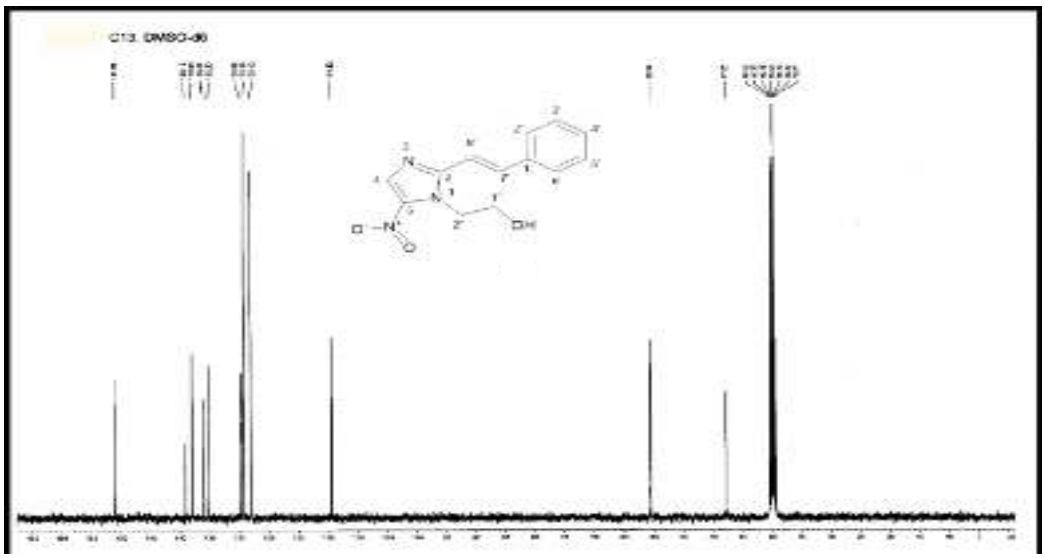

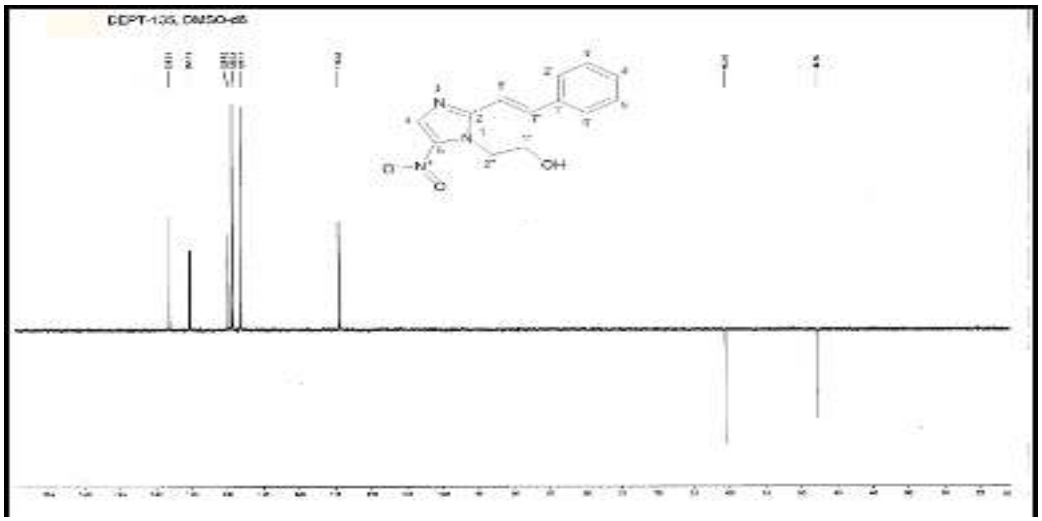

^{1}H, ^{13}C and DEPT-135 NMR spectra of Compound **33**

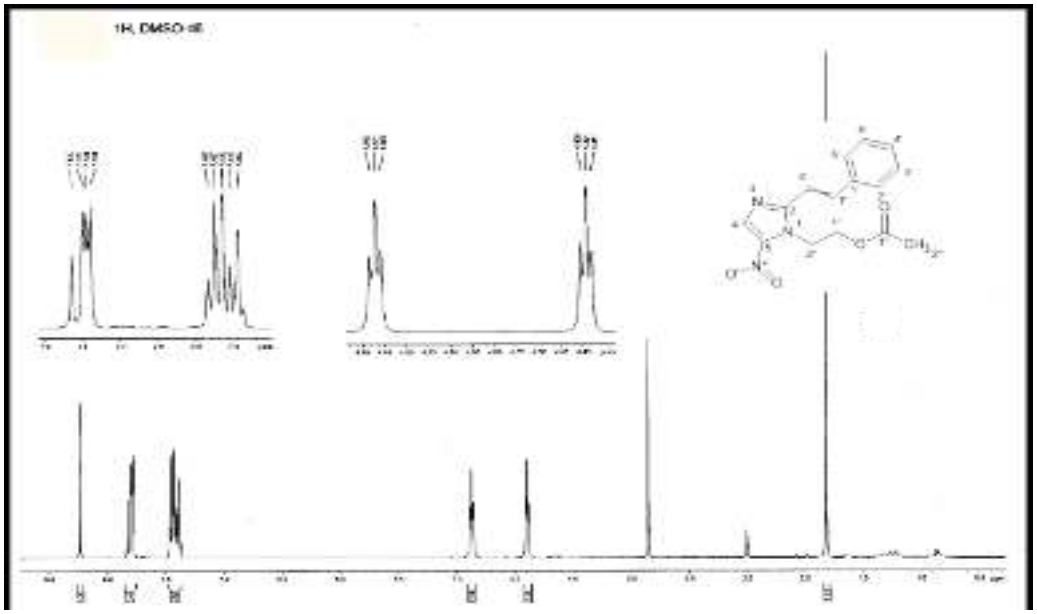

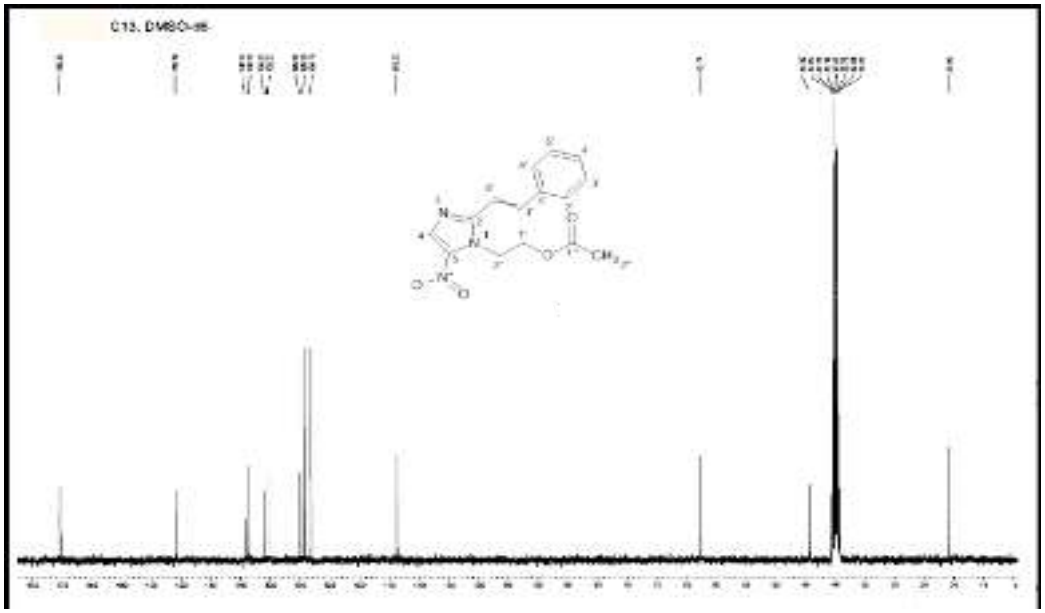

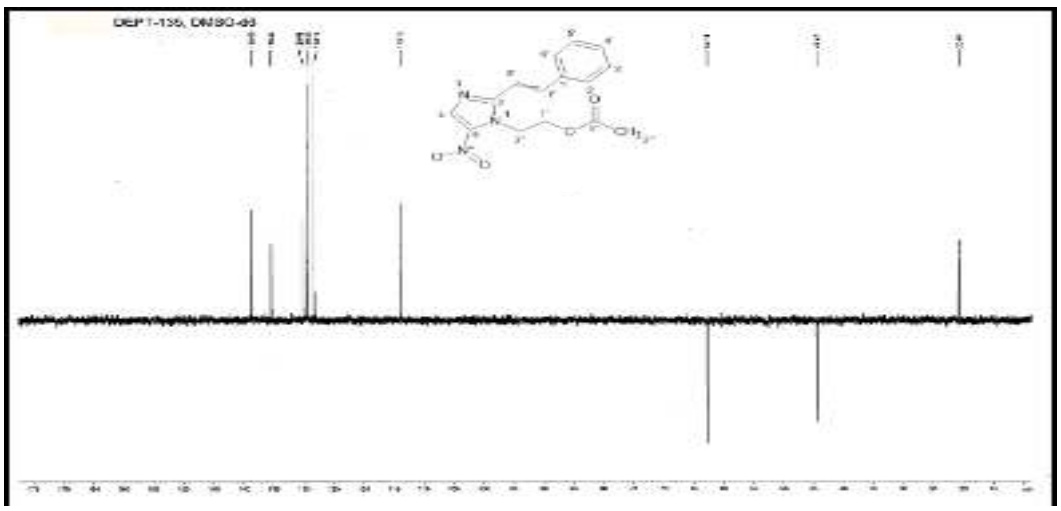

^{1}H, ^{13}C and DEPT-135 NMR spectra of Compound **35**

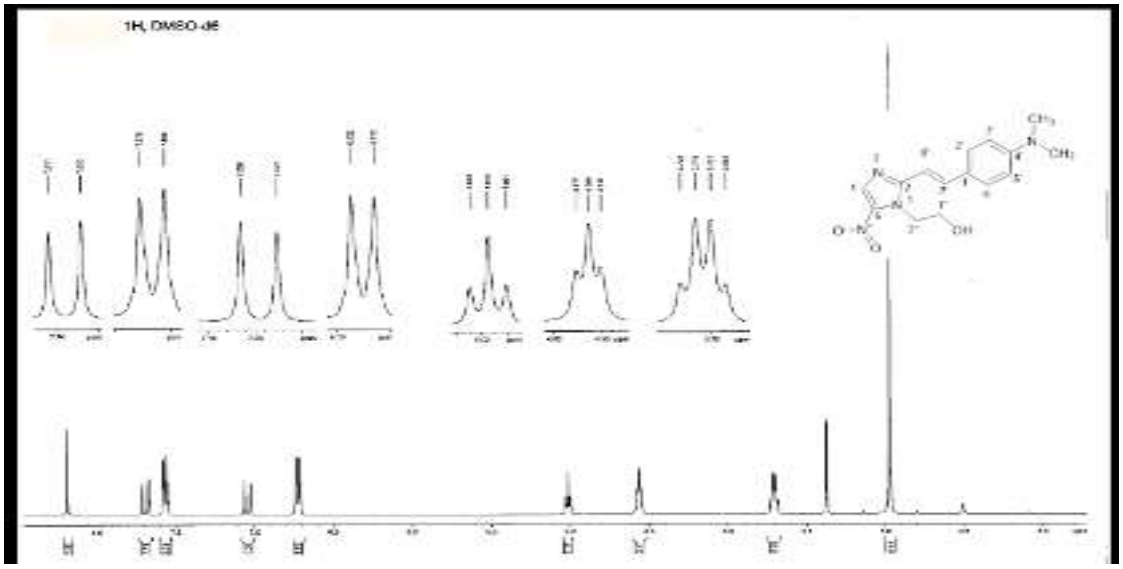

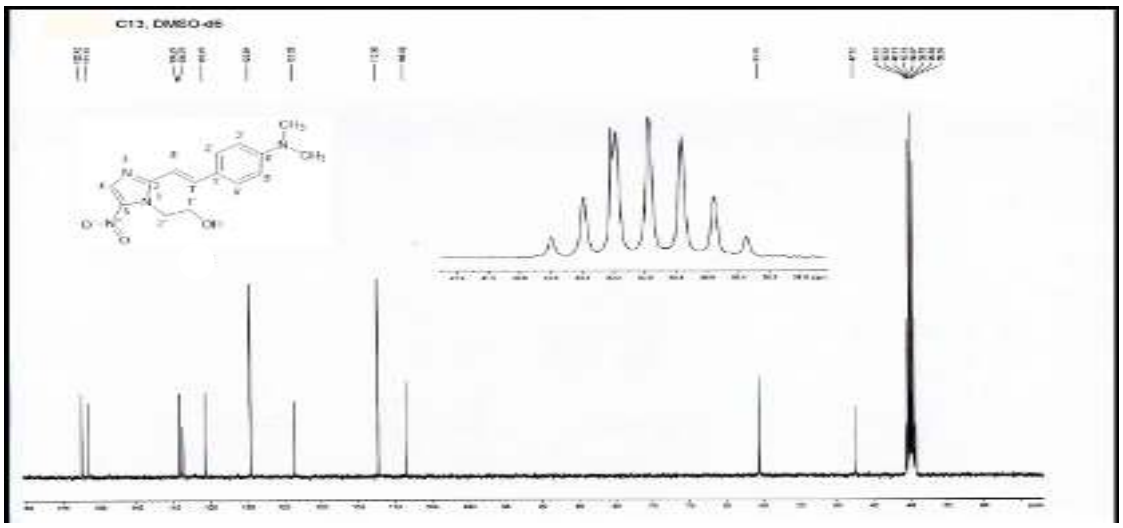

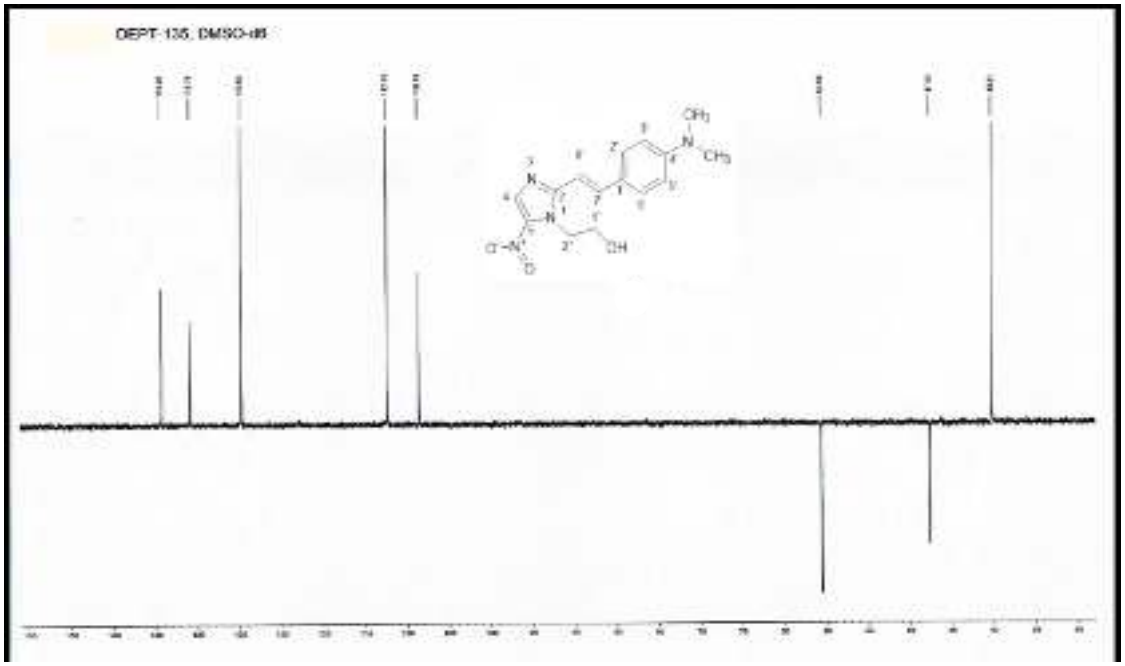

^{1}H, ^{13}C and DEPT-135 NMR spectra of Compound **36**

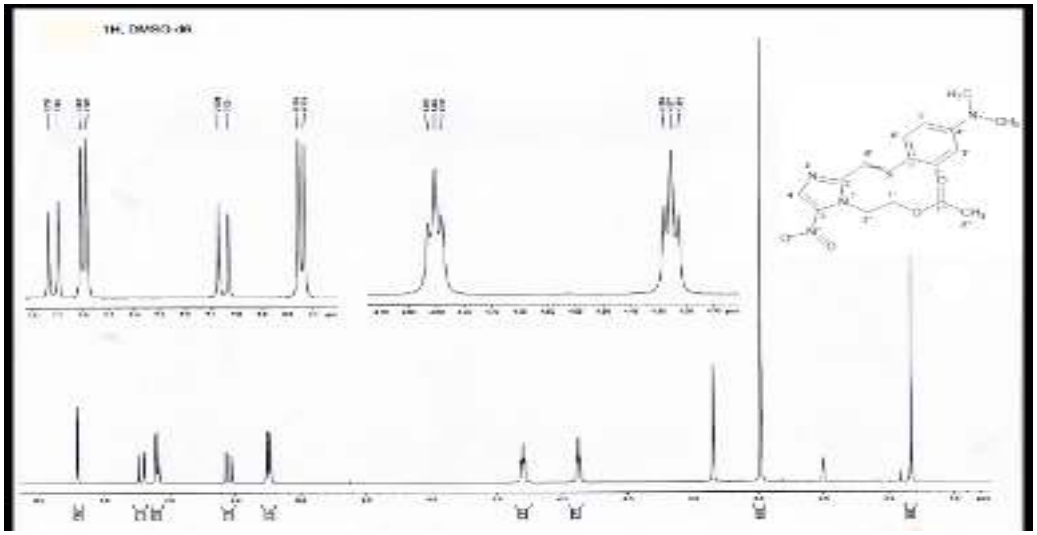

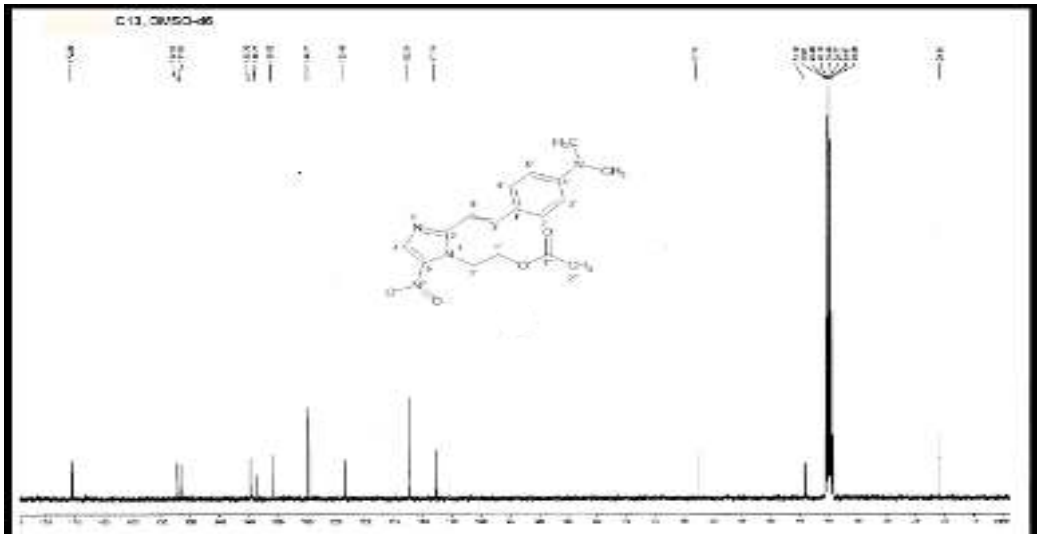

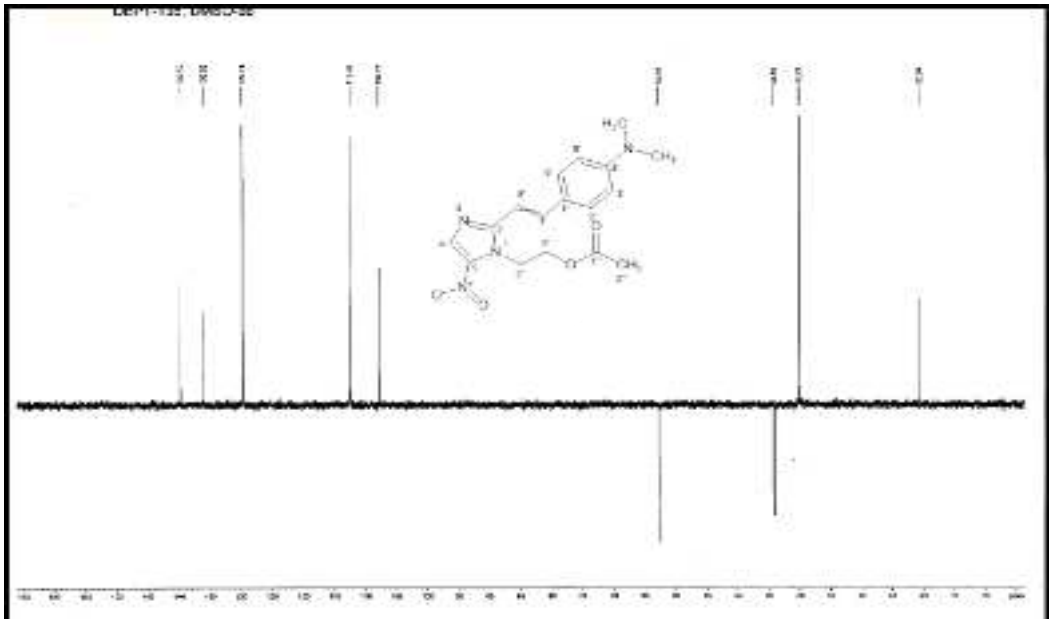

7.2 TLC chromatogram of synthesized compounds

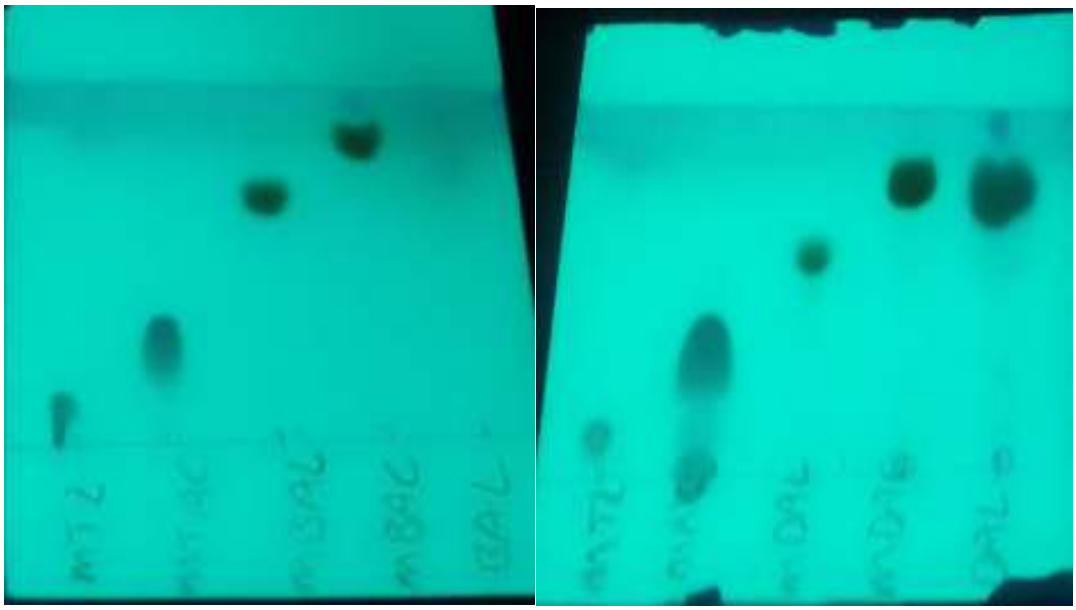

1 2 3 4 5 6

Figures I: Normal phase TLC chromatogram of metronidazole derivatives 1. Metronidazole 2. MTZ Acetate, 3 **Compound 32**, 4. **Compound 33,** 5. **Compound 35,** 6. **Compound 36** viewed under UV 254 light source with the solvent system Chloroform: EtOAc (3:2).

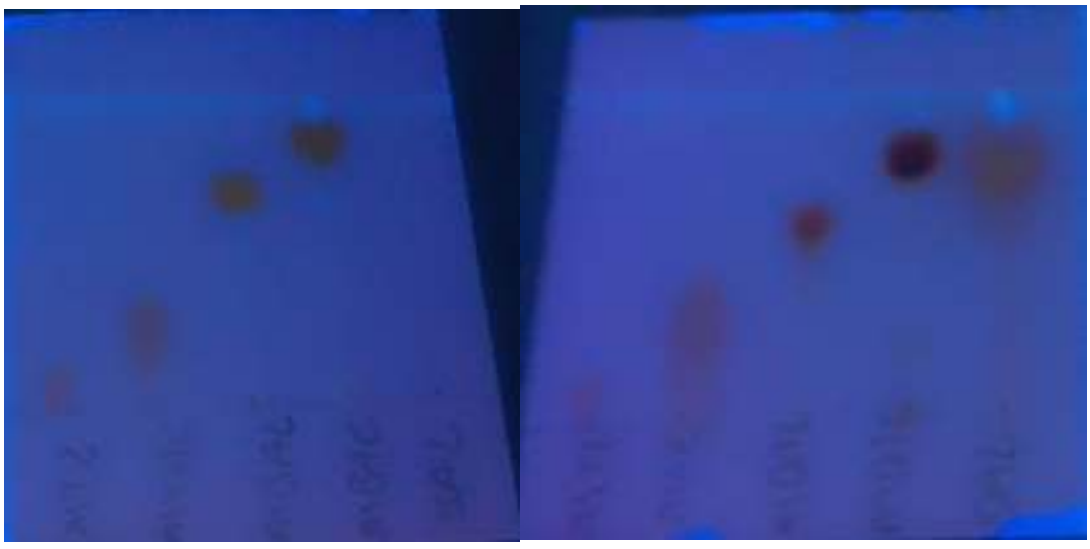

1 2 3 4 5 6

Figures I: Normal phase TLC chromatogram of metronidazole derivatives 1. Metronidazole 2. MTZ Acetate, 3 **Compound 32**, 4. **Compound 33,** 5. **Compound 35,** 6. **Compound 36** viewed under UV 366 light source with the solvent system Chloroform: EtOAc (3:2).

7.3 Pictures of MIC assay of synthesized compounds in 96 micro-well plate

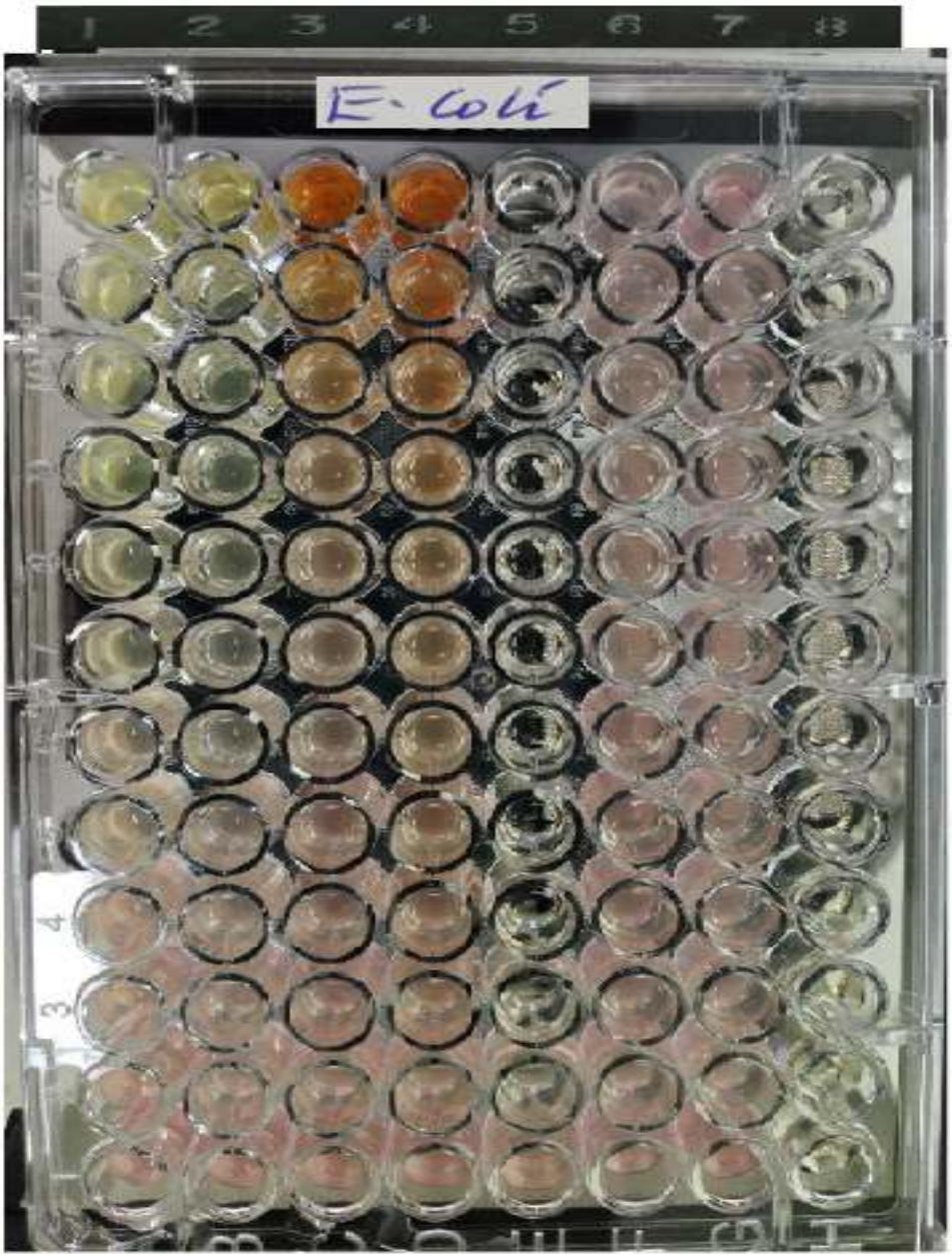

Note: A schematic representation of the 96-well MTT broth microdilution model. Annotations: The yellowish coloration indicates inhibition of growth; purple indicates that organisms are active. 1=compound **33**, 2=compound **32**, 3=compound **35**, 4=compound **36**, 5=positive control (Ciprofloxacillin), 6=negative control (DMSO), 7=growth control, and 8=positive control (Media)

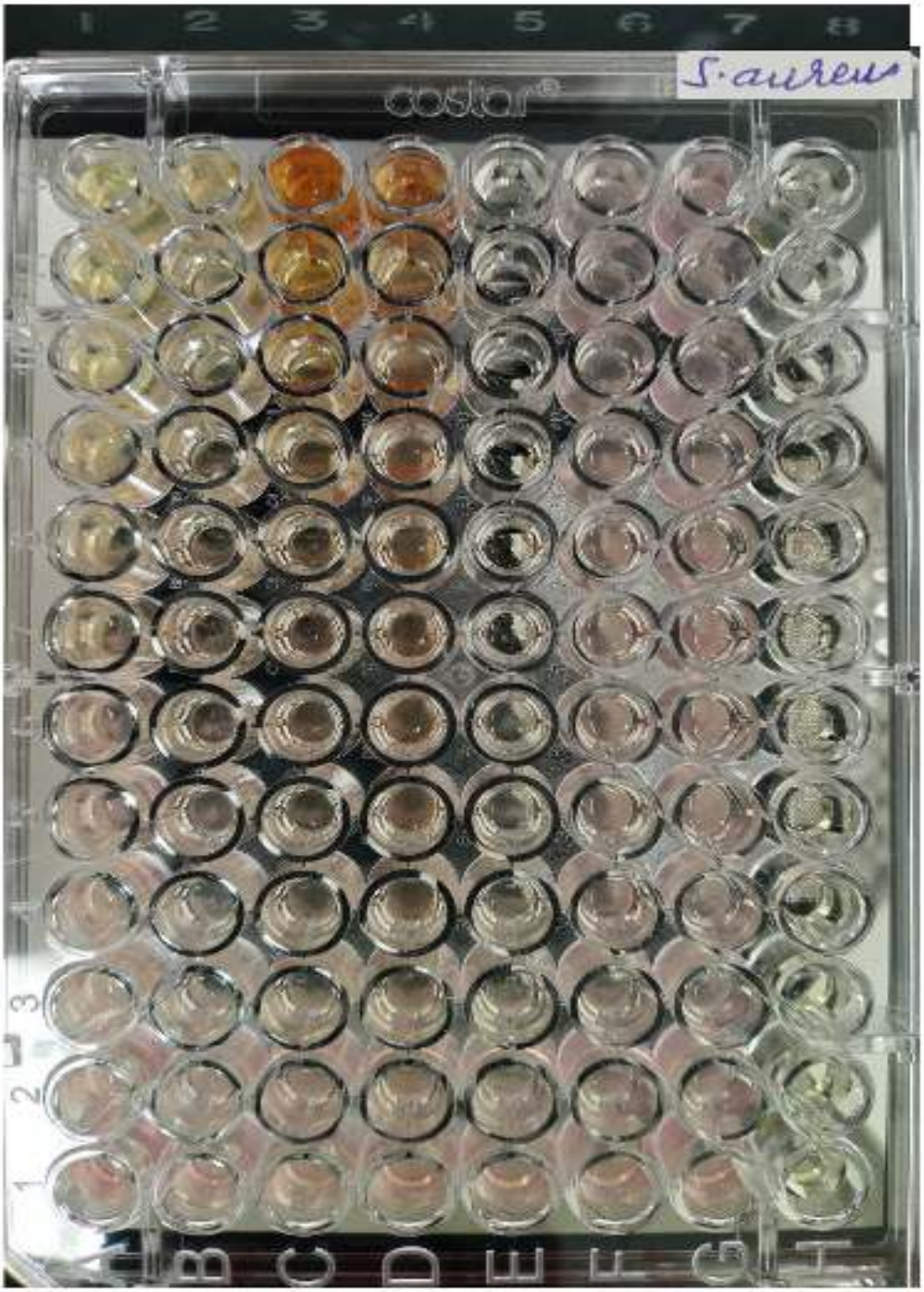
1 2 3 4 5 6 7 8
costar
S. aureus
A B C D E F G H
1
2
3

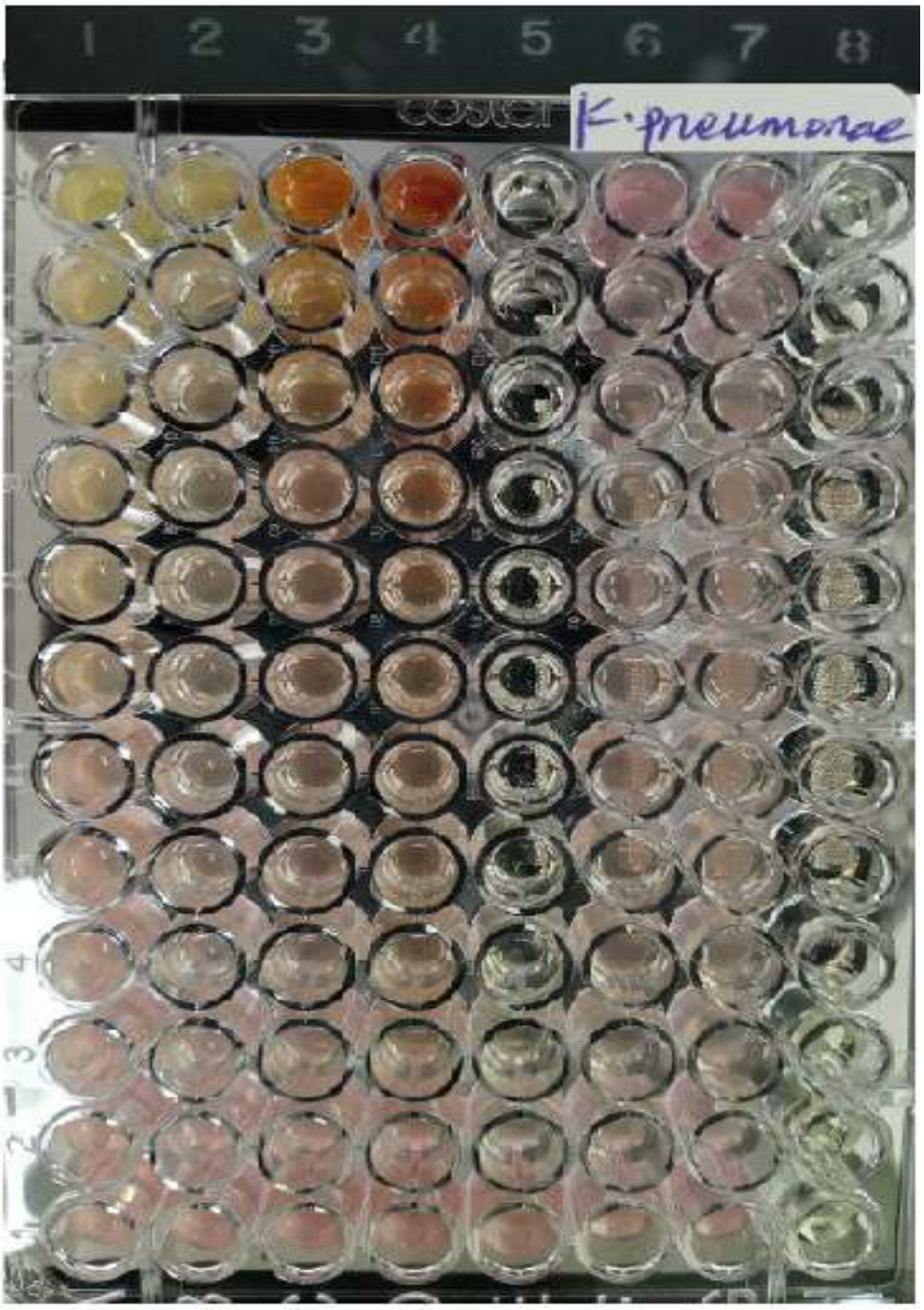
1 2 3 4 5 6 7 8
K. pneumoniae

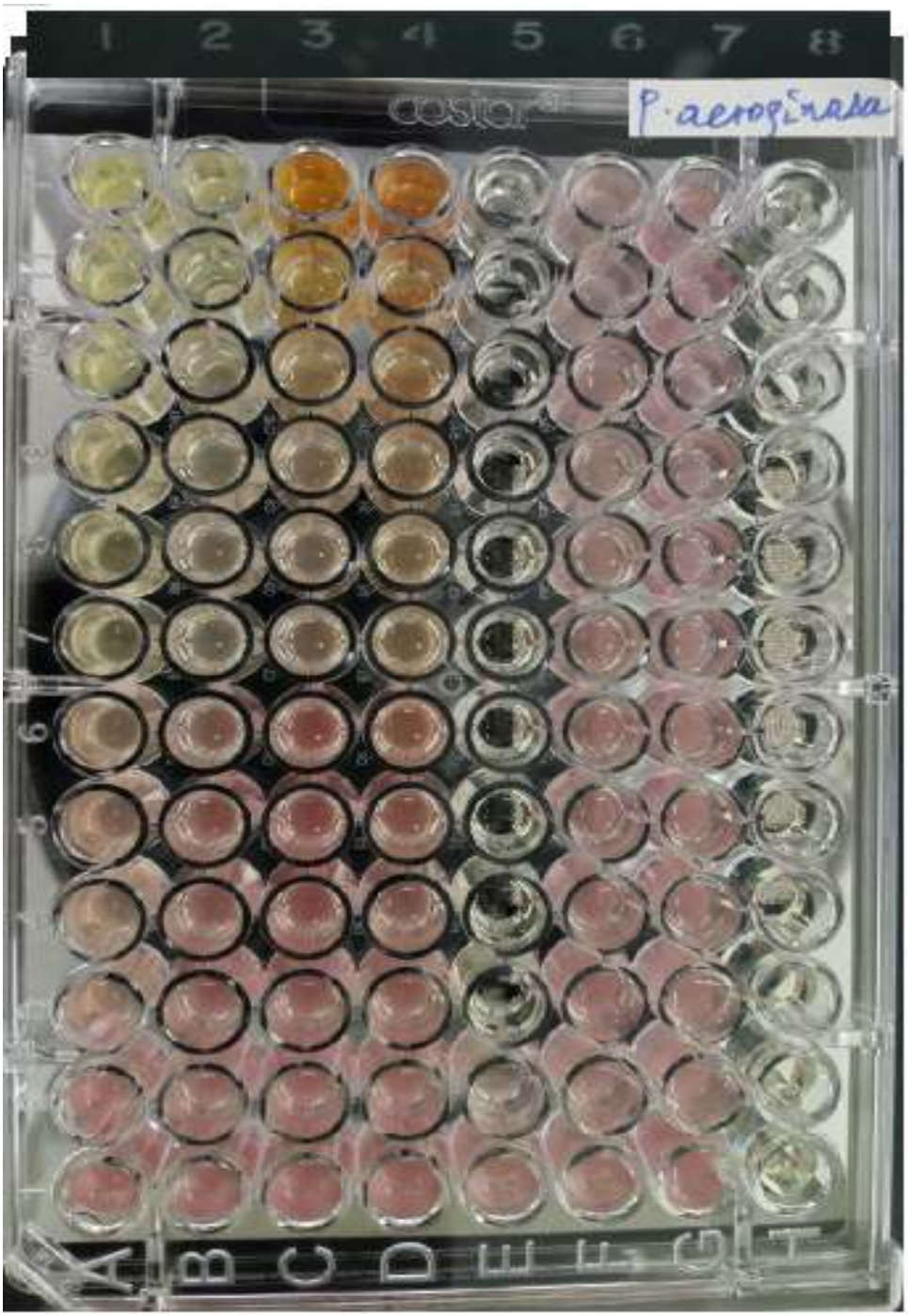
1 2 3 4 5 6 7 8
P. aeruginosa
A B C D E F G H

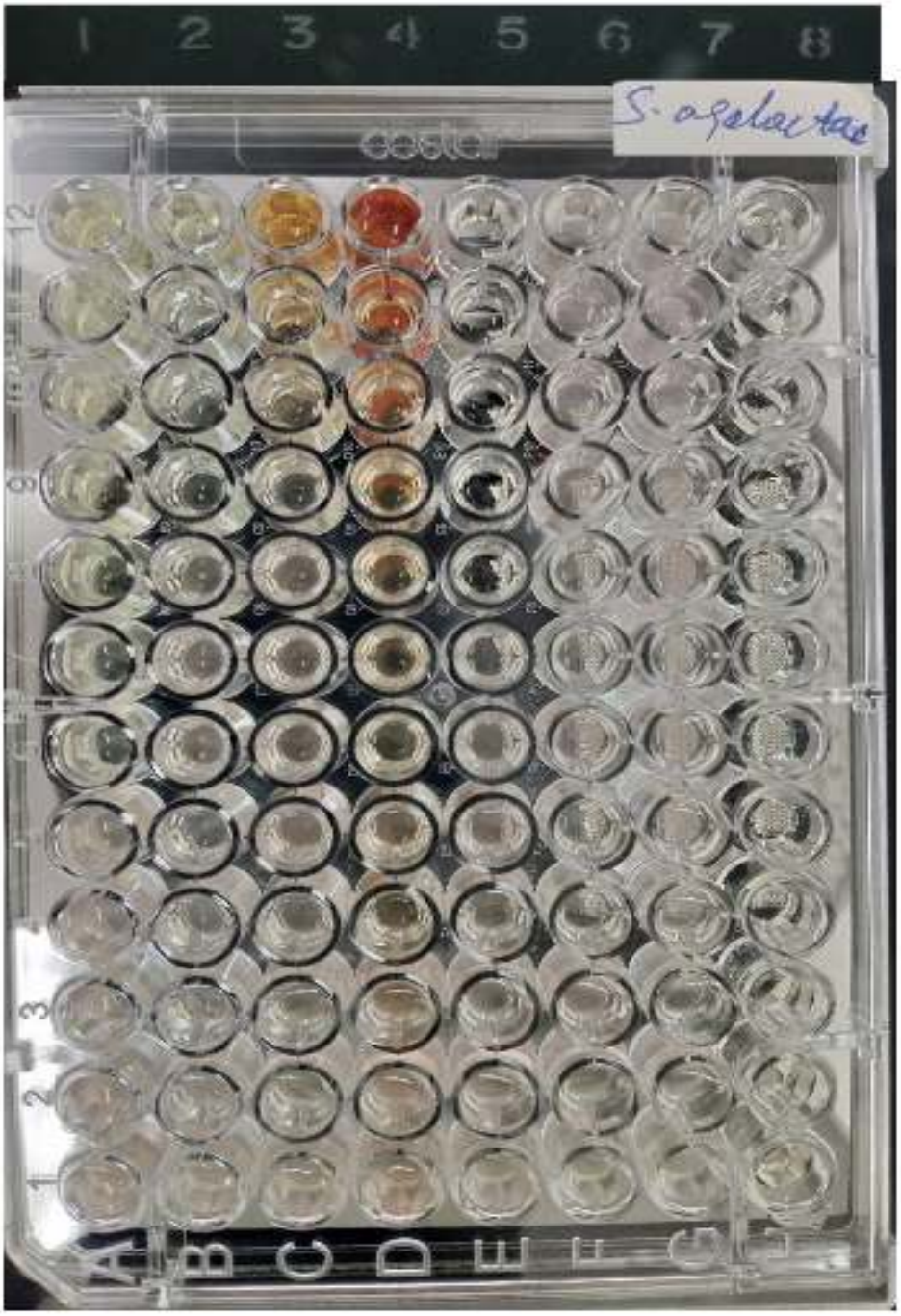
1 2 3 4 5 6 7 8
S. agalactiae

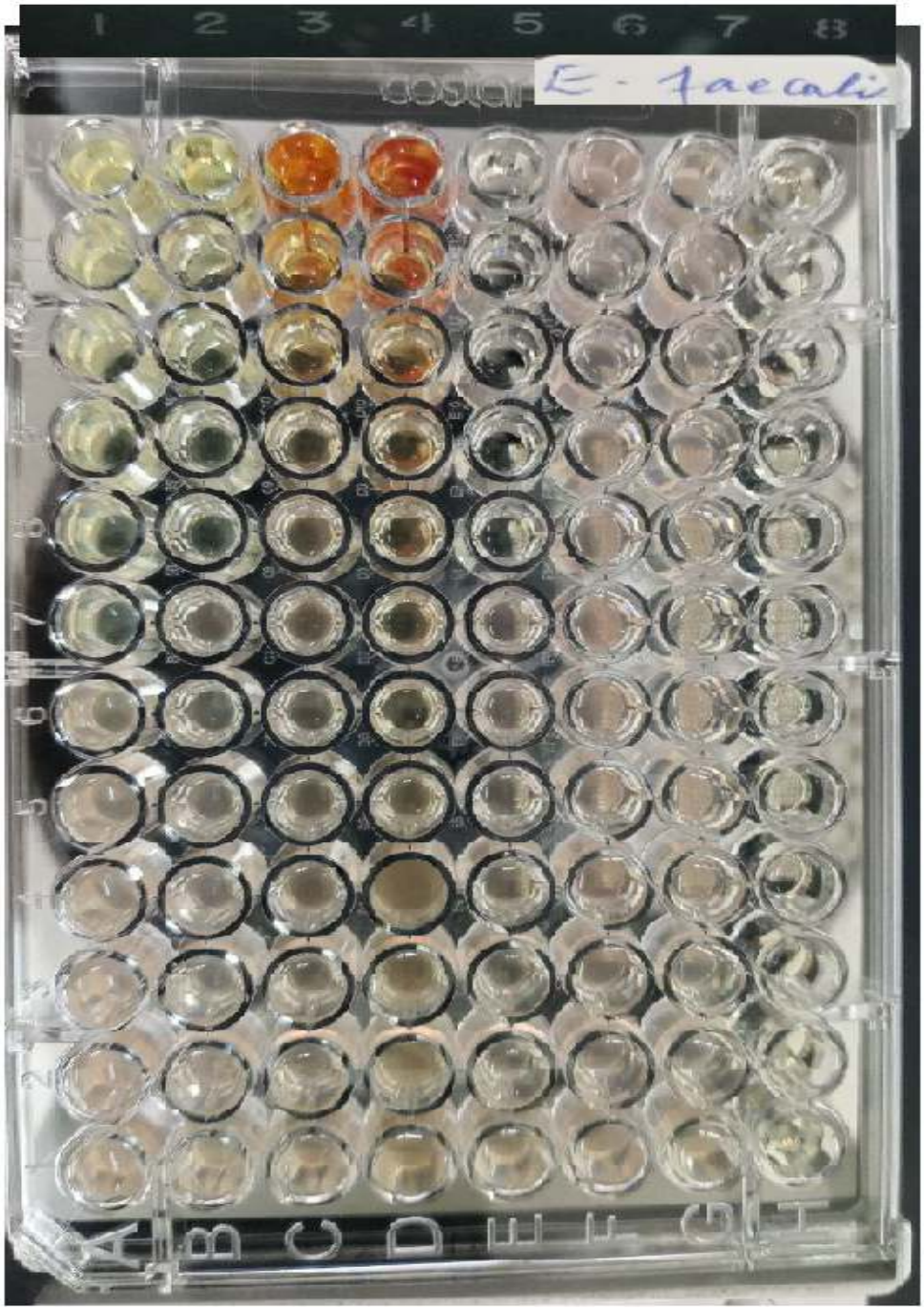
1 2 3 4 5 6 7 8
E. faecalis
A B C D E F G H

7.4 Binding Interaction of synthesized compounds in *E. coli* FabH (1HNJ.pdb)

Compound 33

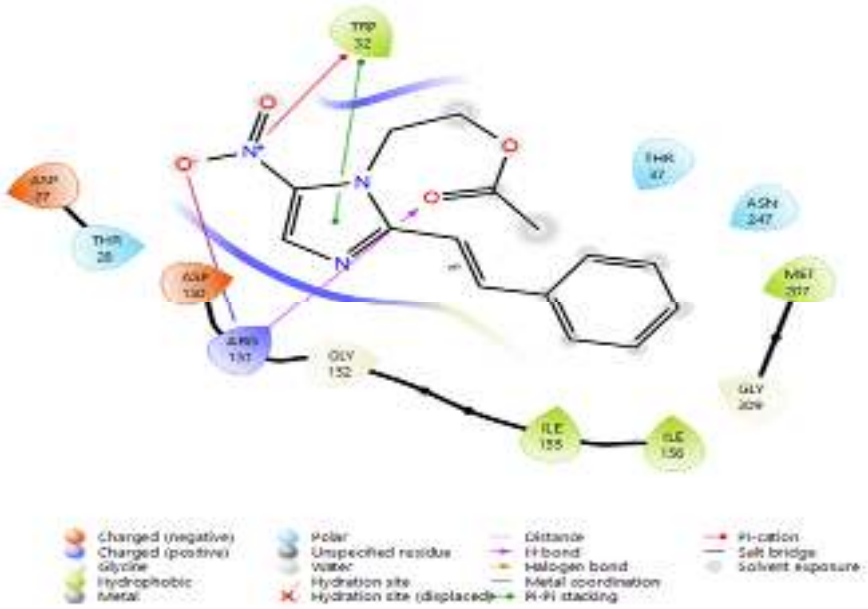

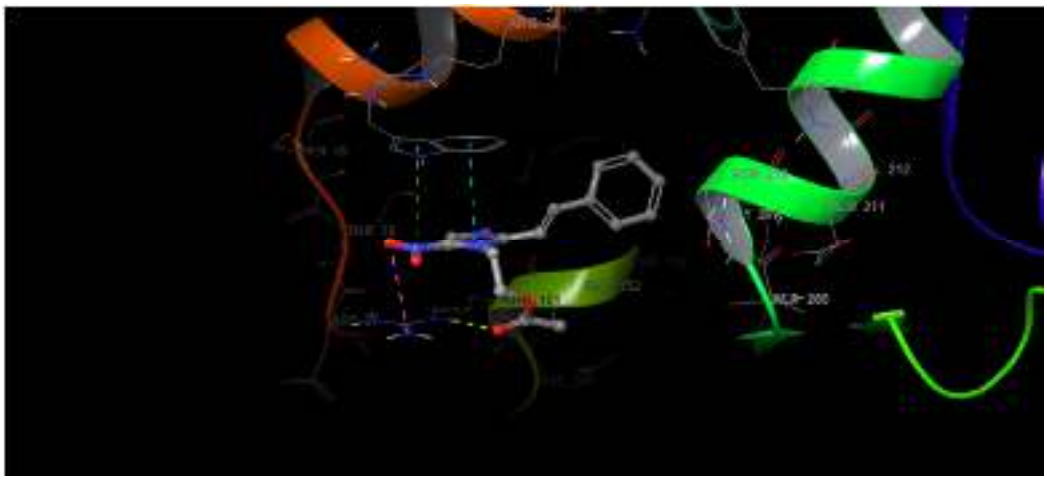

Compound 36

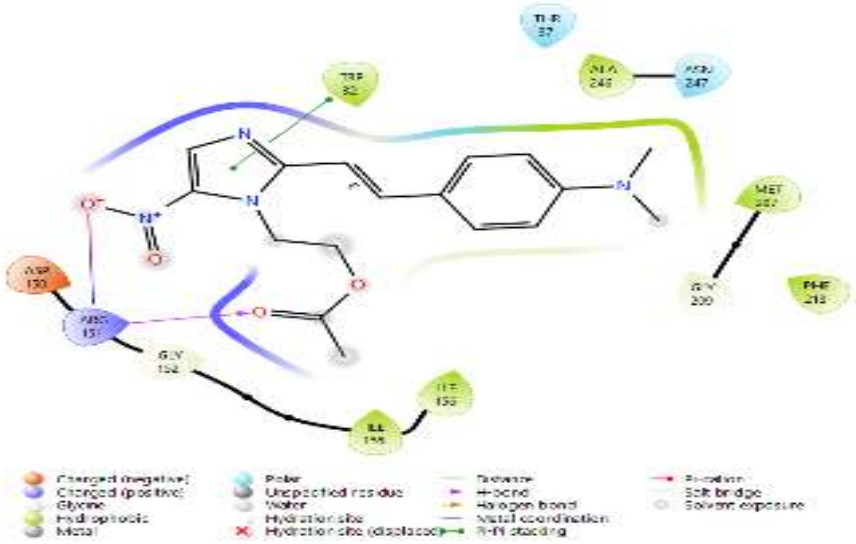

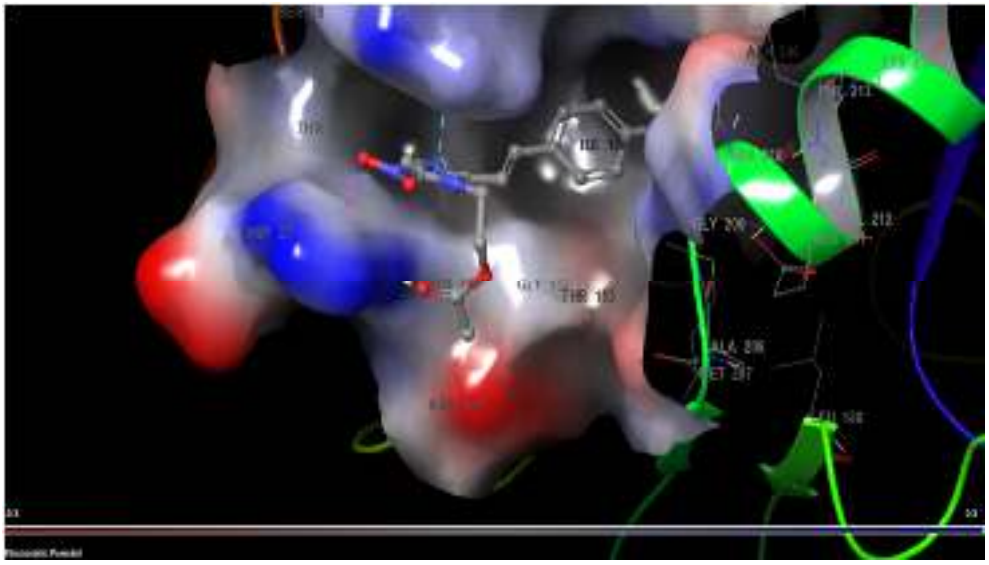

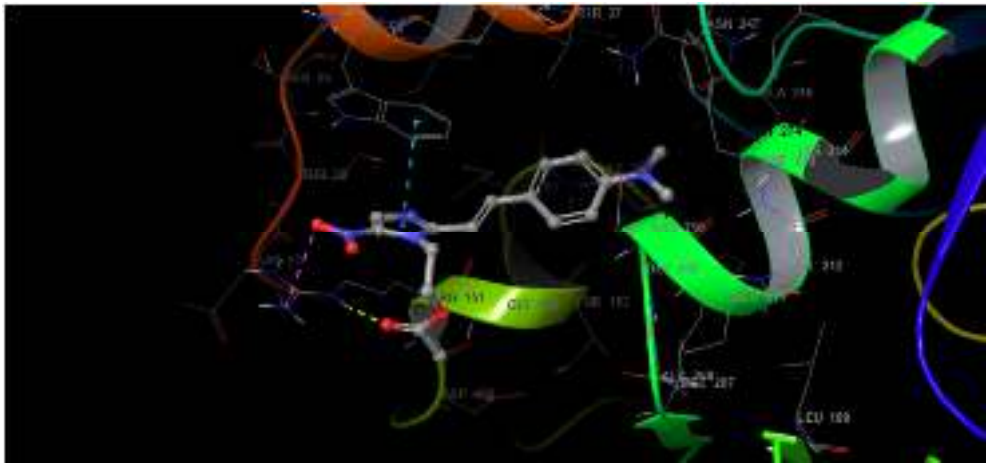

Compound 35

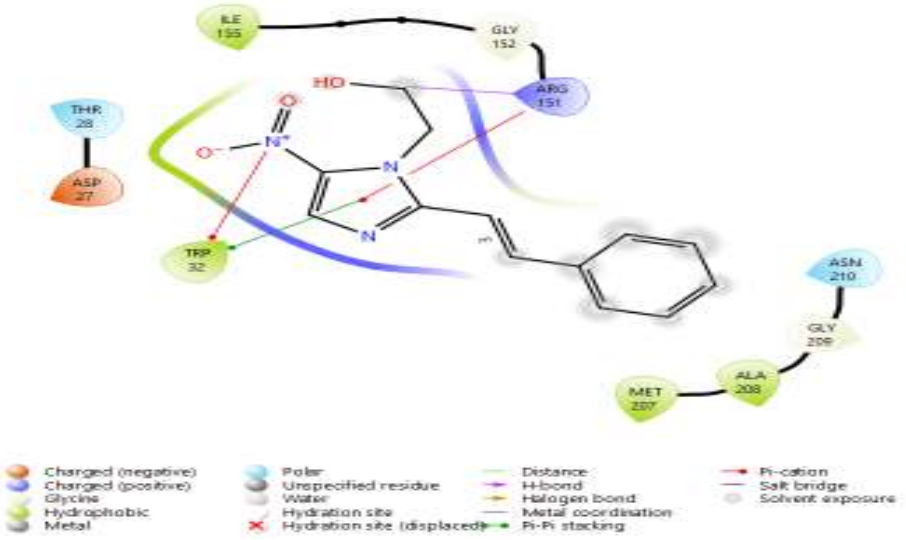
ILE 155
GLY 152
ARG 151
HO
O
O⁻
N⁺
N
N
THR 28
ASP 27
TRP 32
ASN 210
GLY 209
ALA 208
MET 207
Charged (negative)
Charged (positive)
Glycine
Hydrophobic
Metal
Polar
Unspecified residue
Water
Hydration site
Hydration site (displaced)
Distance
H-bond
Halogen bond
Metal coordination
Pi-Pi stacking
Pi-cation
Salt bridge
Solvent exposure

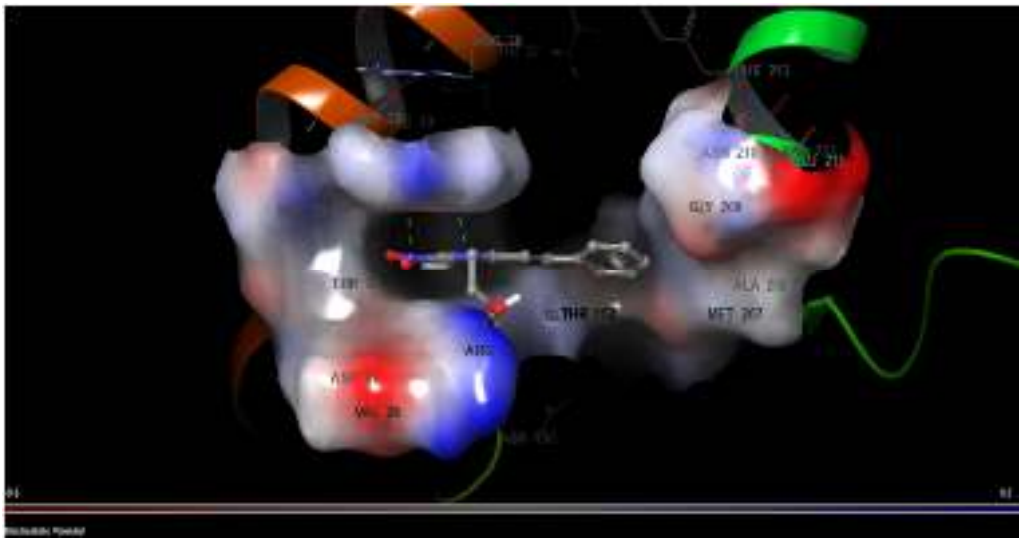

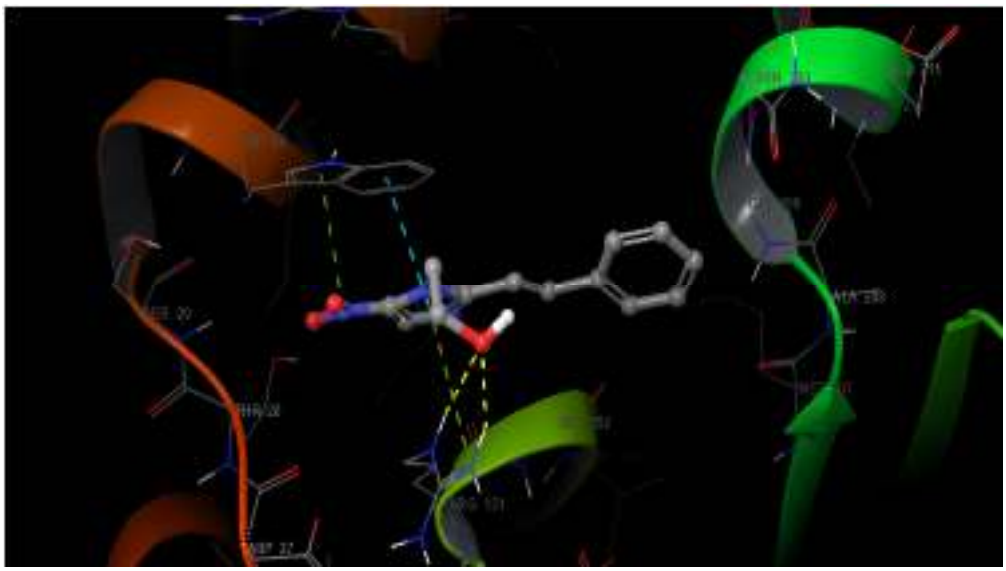

Compound 36